N-acylated Rab5b GTPase and Downstream Binding Proteins Regulate Specific Membrane Traffic in Blood-stage Malaria Parasites

January 2022

Izumi TAKU

N-acylated Rab5b GTPase and Downstream Binding Proteins Regulate Specific Membrane Traffic in Blood-stage Malaria Parasites

A Dissertation Submitted to
the Graduate School of Life and Environmental Sciences,
the University of Tsukuba
in Partial Fulfillment of the Requirements
for the Degree of Philosophy in Science
Doctoral Program in Biological Sciences

Izumi TAKU

Table of contents

Abstract

Newly synthesized secretory proteins are transported from the endoplasmic reticulum (ER) via the Golgi apparatus to be delivered to plasma membrane. Sar1 GTPase plays a critical role as a molecular switch for the cargo sorting at the ER. Arf and Rab GTPases regulate protein transport at the Golgi apparatus. All small GTPases are activated by a guanine nucleotide exchange factor (GEF), and activated GTPases recruit specific effectors to regulate downstream reaction. These discoveries are mainly reported from human and yeast, and findings from protozoan parasite has been limited.

Plasmodium parasites, the causative agents of malaria, export hundreds of parasite proteins toward host erythrocytes membrane. Many of exported proteins possess a conserved *Plasmodium* export element (PEXEL), whereas PEXEL negative proteins (PNEPs) are also exported. Currently, how small GTPases regulate the transport of export proteins remains poorly understood.

N-acylated Rab5 isotype, called Rab5b, localizes at adjacent to the ER and regulates export of *Plasmodium falciparum* adenylate kinase 2 (PfAK2), which is one of PNEPs and possesses N-acylation. To elucidate the mechanism how PfRab5b regulates the export of PfAK2, three candidates of PfRab5b binding proteins have been isolated: PfArf1, PfRab1b, and Arf1 GEF, PfSec7. In this study, I characterized the role of three candidate proteins on the cargo selection in *Plasmodium*.

First, sub-cellular localization of Sec7 was analyzed. I used rodent malaria parasite *P. berghei* with the advantage of genetic recombination into chromosomes. PbSec7 formed dimer in the parasite cytosol, and specific amino acids required for the dimerization were conserved in PbSec7. Although Arf1, Rab1b and Sec7 are localized to the Golgi in other organisms, PbSec7 was localized to the close to the ER. Colocalization of PbSec7 with PbRab5b or PbArf1 were also observed. These results were the first report from *P. berghei*.

Next, detailed localization of Arf1 and Rab1b was observed in *P. falciparum*. A super-resolution microgram revealed that the ER marker PfBiP was located closer to PfArf1 than to PfRab1b, suggesting that the two GTPases localized to different ER subdomains. The expression of an active or inactive PfArf1 mutant specifically inhibited the export of PfAK2 to the parasitophorous vacuole membrane, while expression of the inactive PfArf1 or PfRab1b mutant decreased the export of PEXEL-positive Rifin. These results suggest that PfArf1 is extensively involved in the transport of PfAK2, and PfArf1 and PfRab1b are involved in the transport of Rifin, indicating the sequential roles of PfArf1 and PfRab1b in cargo selection.

This work is the first report on the cargo selection on the different ER subdomain by three GTPase, PfRab5b, PfArf1 and PfRab1b, via Sec7, and is unique to *Plasmodium* spp. My findings also indicated the diversity of trafficking system mediated by Rab GTPases in eukaryotes.

General Introduction

0-1 Membrane traffic in the eukaryotic cell

In the process of evolution, eukaryotic cells developed complicated membrane structures which compartmentalize organelles and vesicles. These membranes enclose various materials including proteins and traffic in the cell by moving dynamically. This phenomenon is called “Membrane traffic” and highly conserved in all eukaryotes (Nakayama, 2004). The membrane traffic is categorized into four pathways: secretory pathway, biosynthesis pathway, endocytosis pathway and autophagy pathway. All pathways play essential roles to maintain biological function in a eukaryotic cell and various diseases will be caused by collapse to maintain cell function, even if a small part of the membrane traffic failed (Yarwood et al., 2020). Especially, the secretory pathway plays fundamental roles in eukaryotic cells. In the secretory pathway, newly synthesized proteins which possess signal peptide at the N-terminus are transported from the endoplasmic reticulum (ER) to the Golgi apparatus (Viotti, 2016). The cargo proteins are processed by glycosylation at the Golgi apparatus and sorted to various destination like plasma membrane at the trans-Golgi network, then transported to plasma membrane and outside of the cell (Viotti, 2016). Protein transport consists three steps: cargo sorting and vesicle budding at the donor organelle, vesicle trafficking from the donor organelle to the acceptor organelle, vesicle docking and fusion at the acceptor organelle. Cargo proteins

are transported to the destination by repeating these three steps and many molecules are involved in regulation of membrane traffic. For instance, SNARE complex, AP complex and small GTPases classified as Sar/Arf and Rab families play main role to mediate transporting proteins (Scales et al., 2000; D'Souza-Schorey and Chavrier, 2006; Stenmark, 2009; Wang et al., 2017).

0-2 Small GTPases as a key regulator of membrane traffic

Secretory proteins are synthesized in the endoplasmic reticulum (ER) and are delivered to their destinations via the Golgi apparatus. ER-to-Golgi trafficking is highly conserved among eukaryotes, and two types of Ras super families of GTPases, the Sar/Arf and Rab families, mediate protein sorting and transport as molecular switches between these organelles (Suda et al., 2018; Kurokawa and Nakano, 2019). A guanine nucleotide exchange factor (GEF) acts on GDP-bound form of GTPase to convert it to a GTP-bound active state, and a GTPase accelerating protein (GAP) binds to the GTPase to catalyze hydrolysis of the bound GTP to GDP and thereby convert the GTPase back to its inactive state (Hutagalung and Novick, 2011). The GTPase cycle between GDP-and GTP-bound forms causes conformational changes and specific effector molecules are recruited to the GTP-bound active form to complete various membrane trafficking events (Stenmark, 2009; Donaldson and Jackson, 2011). Many regulatory functions performed by the

proteins in the Sar/Arf and Rab families were identified by their interaction with diverse effector proteins that select cargo, promote vesicle movement, and verify the correct site for fusion (Hutagalung and Novick, 2011).

The Sar/Arf and Rab families of GTPases regulate the bidirectional transport between ER and the Golgi in mammalian cells and land plants (Brandizzi and Barlowe, 2013). Newly synthesized secretory proteins translocate into the ER lumen using the N-terminal signal peptide (Nickel and Rabouille, 2009). The ER luminal chaperone BiP assists in folding newly synthesized proteins to maintain protein homeostasis (Craig et al., 1993). Activation of the ER-localized GTPase Sar1 and its GTP hydrolysis triggers the recruitment of the COPII coat component and causes the enrichment of cargo proteins into the ER exit sites (ERES) where COPII-coated vesicles form (Kung et al., 2012; Yorimitsu and Sato, 2012). The COPII machinery performs two critical functions: first, Sar1 and the inner layer Sec23-Sec24 COPII subunits bind to and select specific cargo for packaging; second, polymerization of the outer layer of Sec13-Sec31 COPII subunits occurs into a cage structure to drive vesicle formation (Bi et al., 2007). After uncoating of the COPII coat, diffusive vesicles are anchored to cis-Golgi membranes by the extended coiled-coil domain that tethers factor protein p115, the yeast homolog of Uso1, as well as the multi-subunit TRAPPI (transport protein particle I) complex that activates Rab1 GTPase (Cai et al., 2007). The fusion of vesicles depends on the assembly of

integral membrane SNARE complexes between the donor and acceptor membranes (Allan et al., 2000). In contrast, a heptameric complex COPI-coated vesicle facilitates the retrieval of escaped ER luminal proteins that contain KDEL signals, which are recognized by the resident KDEL receptor ERD2 in the cis-Golgi, and by SNARE proteins (Lewis et al., 1990; Semenza et al., 1990). Once Arf1 is activated by the GEF which contains a conserved Sec7 domain, the membrane-localized Arf1 recruits the COPI coat to the cis-Golgi membranes (Zhao et al., 1999). The COPI subunits recognize the sorting motifs of transmembrane cargo proteins and are incorporated into nascent COPI vesicles and subsequently retrieve cargo proteins to the ER (Eugster et al., 2000). Most Rab and Arf GTPases carry lipid modifications that are necessary for membrane recruitment. In the case of Rab, a carboxy-terminal geranylgeranylation (20-carbon unsaturated fatty acid) group at the C-terminal cysteine residue is responsible for the membrane attachment of the Rab-GTP form (Leung et al., 2006). In contrast, the N-terminal glycine residue of Arf is myristoylated (14-carbon saturated fatty acids) (Pasqualato et al., 2002).

0-3 Malaria and the malaria parasite

Malaria is one of the most severe disease and counted in three major infectious diseases of the world with tuberculosis and acquired immunodeficiency syndrome (AIDS). According to the World Malaria Report 2020 reported from WHO, there were about 230

million cases and 409,000 deaths in 2019. Malaria is prevalent in 87 countries, mainly in tropical and subtropical regions (WHO, 2020). The protozoan parasite the genus *Plasmodium* is the causative agent of malaria and it is transmitted by the Anopheline mosquito. Five species of *Plasmodium* spp. infect human: *P. falciparum*, *P. vivax*, *P. ovale*, *P. malariae* and *P. knowlesi*. These malaria parasites proliferate drastically in human liver cell and start proliferate in human erythrocytes. Proliferating parasites in human erythrocytes cause the malaria symptoms including fever, anemia and splenomegaly. Especially, *P. falciparum* cause lethal symptoms, for instance, malarial nephropathy and cerebral malaria. Therefore, it is important to understand the behavior of *Plasmodium* parasites in human erythrocytes.

0-4 Protein secretion in the malaria parasite

Plasmodium falciparum extensively remodels the human erythrocytes in which it resides (de Koning-Ward et al., 2016). The remodeling process is conducted by hundreds of proteins exported from the parasites into the host cell compartment, and these enable virulence-related functions including cytoadherence to the vascular endothelium, immune evasion, and nutrient uptake (Miller et al., 2013). Many of the exported proteins contain a five amino acid motif termed the *Plasmodium* export element (PEXEL) which is found ~20 amino acids downstream of the signal peptide (Hiller et al., 2004; Marti et al., 2004).

The PEXEL motif is removed in the ER lumen of the parasite by the ER resident aspartic protease plasmepsin V before exit of the ER (Boddey et al., 2010; Russo et al., 2010). All repertoires of COPII and COPI components are conserved in the *Plasmodium* spp. (Kibria et al., 2019), suggesting that the early secretory system of *Plasmodium* may resemble that in higher eukaryotes. Several studies have reported that the fungal metabolite brefeldin A (BFA), which inhibits the Golgi-localized GEF Arf1, disrupts the accurate export of PEXEL-containing proteins (Akompong et al., 2002; Chang et al., 2008), indicating that these proteins are trafficked through the classical ER-Golgi pathway. Subsequently, the exported proteins are transported across the parasite plasma membrane and the parasitophorous vacuole membrane (PVM) via the multimeric *Plasmodium* translocon of exported proteins (PTEX) into the erythrocyte cytosol (de Koning-Ward et al., 2009).

Several exported proteins lacking an N-terminal PEXEL motif and are called PEXEL-negative proteins (PNEPs). These also translocate through PTEX for export into the erythrocyte cytosol (Spielmann and Gilberger, 2010; Elsworth et al., 2014). For example, the skeleton binding protein 1 (SBP1), which is a PEXEL-negative transmembrane protein, is supposed to export via the classical secretory pathway, because the truncated SBP1 internalized in the perinuclear staining corresponding to the ER (Saridaki et al., 2009). However, recent report that SBP1 was included within electron-dense materials in the parasite cytoplasm (Iriko et al., 2020), strongly suggests that the presence of alternate

export pathways except for the classical ER-to-Golgi transport pathway in the parasite trafficking system.

In these *Plasmodium* trafficking systems, the roles of small GTPases are poorly understood such that the subcellular localization and function of only one Sar1 and six Rab GTPases has been being characterized functionally; i.e., PfSar1, PfRab1a, PfRab5a, PfRab5b, PfRab6, PfRab7, and PfRab11a (Adisa et al., 2001; Struck et al., 2005; Elliott et al., 2008; Agop-Nersesian et al., 2009; Rached et al., 2012; Krai et al., 2014; Ebine et al., 2016; Morse et al., 2016). However, effectors and binding proteins have only been identified for PfRab11a (Agop-Nersesian et al., 2009). Further, PfRab11a is associated with the myosin-tail-interacting-protein and is crucial for the parasite invasion of host cells (Agop-Nersesian et al., 2009).

0-5 N-acylated Rab5b, a unique small GTPase in the malaria parasite

Almost all Rab GTPases are geranylgeranylated at the cysteine residue in the C-terminal region for membrane attachment of the Rab-GTP form in eukaryotic cell (Leung et al., 2006). In *Plasmodium* spp., 11 Rab GTPase are conserved: Rab1a, Rab1b, Rab2, Rab5a, Rab5b, Rab5c, Rab6, Rab7, Rab11a, Rab11b and Rab18 (Kremer et al., 2013). All Rab GTPases, except for *Plasmodium* Rab5b, are modified with geranylgeranylation same as other eukaryotic cell, however, Rab5b modified with myristoylation (14-carbon) and

palmitoylation (16-carbon saturated fatty acid) at the N-terminal glycine and cysteine residues, respectively (Ezougou et al., 2014; Ebine et al., 2016). In rodent malaria *P. berghei*, gene-deletion of PbRab5b was unsuccessful, indicating *Plasmodium* Rab5 is essential for the blood stage growth (Ezougou et al., 2014; Ebine et al., 2016). Subcellular localization of PfRab5b is proximal to the region of the BiP-positive ER, and segregated from COPII subunit Sec13-positive ERES (Ebine et al., 2016). PfRab5b mainly localized adjacent to the ER, but the secretion of PfRab5b observed from the parasite cytoplasm to the RBC-cytoplasmic face of the PVM (Ebine et al., 2016). Interestingly, *Plasmodium falciparum* adenylate kinase 2 (PfAK2), which lacks a signal peptide and the PEXEL motif, but retaining the N-terminal myristoylation and palmitoylation motif that is similar to PfRab5b, were inhibited exporting to the PVM by the overexpression of PfRab5b, however the export of neither the PEXEL-positive erythrocyte vesicle protein 1 (PfEVP1) nor SBP1 were inhibited (Ebine et al., 2016). These findings suggested that PfRab5b may regulate the transport of PfAK2 by the COPII independent non-classical pathway (Ebine et al., 2016).

Currently, none of GTPase, which regulates the trafficking of PNEPs including PfAK2, is elucidated. A bioinformatic technique previously identified casein kinase1 as a PfRab5b binding protein (Rached et al., 2012); however, it remains unclear how PfRab5b is involved in the selective export of PfAK2. To understand the mechanisms underlying the

PfRab5b-dependent specific export pathway, PfRab5b associated proteins were isolated by using coimmunoprecipitation and mass analysis approaches (Hirai, 2016). Lysates prepared from PfRab5b expressing parasites, which were C-terminally fused with the YFP and FLAG-tags (PfRab5b-YFP-FLAG) or a negative control PfRab5b-YFP, were immunoprecipitated with an anti-FLAG antibody and eluted using the FLAG peptide. The eluted samples were analyzed via LC-ToF MS/MS, and 677 peptides were identified from the PfRab5b-YFP-FLAG expressing lysate (Hirai, 2016). Five candidate proteins showing a 3.5–fold change in the expression of PfRab5b-YFP-FLAG relative to PfRab5b-YFP were obtained. These included the ADP-ribosylation factor (PfArf GTPase) (PF3D7_1020900), protein transport protein SEC7 (PfSec7) (PF3D7_1442900), early transcribed membrane protein 10.2 (ETRAMP10.2) (PF3D7_1033200), PfRab1b GTPase (PF3D7_0512600), and the PVM protein S16 (Pfs16) (PF3D7_0406200) (Table 0)(Hirai, 2016). Six Sar/Arf proteins are conserved in *P. falciparum* 3D7 genome database (Figure 0A) (Taku et al., 2021). Amino acid sequencing showed that five of these proteins are Arf family GTPases (PF3D7_1020900, PF3D7-1034700, PF3D7_1442000, Pf3D7_0920500, Pf3D7_1316200), and one is a Sar1 homolog (PF3D7_0416800) based on the conserved effector sequence and the overall amino acid identities (Figure 0C). PF3D7_1020900, which was obtained as PfRab5b interacting protein (Table 0) (Hirai, 2016), showed the highest identity (75%) to human Arf1 among the *Plasmodium* and

human Arf families (Figure 0B). Thus, the PfRab5b-associated protein candidate PF3D7_1020900 is a *Plasmodium* Arf1 homolog and was annotated as PfArf1 (GenBank Accession number, BR001667). In other organisms, the Arf1 GTPase, Sec7, and Rab1b are involved in the transport from the cis-Golgi to the ER (Monetta et al., 2007). ETRAMP10.2 is expressed at an early point of the intraerythrocytic stage and is localized at the parasite periphery, which is assumed to be the PVM (Spielmann et al., 2003). The Pfs16 is expressed in gametocytes and is localized at the parasite periphery, similar to ETRAMP10.2 (Bruce et al., 1994).

In this study, I focused on three candidates of PfRab5b associated protein, PfArf1, PfRab1b and PfSec7 which activate PfArf1, and attempted to elucidate the mechanism that PfRab5b mediate PfAK2 export to the PVM by characterizing these three candidates in *Plasmodium* spp. Characterization of *Plasmodium* Sec7 is reported in Chapter 1. Domain structure of *Plasmodium* Sec7 were determined from multiple alignment of Sec7s in eight different *Plasmodium* species. Amino acid residues which are necessary for homodimerization of Sec7s were conserved at N-terminal region of *Plasmodium* Sec7 (Ramaen et al., 2007) and it was confirmed that PbSec7 formed homodimer in parasite by Western analysis using reduced and non-reduced protein samples. Indirect immunofluorescence assay for PbSec7-mCherry expressing parasite revealed that PbSec7 localized adjacent to the ER in some population of parasites. Colocalization of PbSec7

with PbArf1 or PbRab5b were also observed in dual expressing parasites. These data suggested that PbSec7 may interact with PbRab5b and PbArf1 and mediate the protein transport at near the ER. Characterization of PfArf1 and PfRab1b is reported in Chapter 2. I found that the PfArf1 and PfRab1b GTPases were colocalized with PfRab5b in the compartment close to the ER. Indirect immunofluorescence assay for PfArf1- or PfRab1b- expressing parasites using super-resolution microscopy revealed that PfArf1 and PfRab1b were localized to different ER subdomains. Further, using a genetic approach to express an active or inactive mutant indicated that PfArf1, but not PfRab1b, was involved in the export of PfAK2 to the PVM. Unexpectedly, PfRab1b participates in the trafficking of the PEXEL-positive export protein Rifin. These data suggest that the export pathways of PfAK2 and Rifin are separated in the PfArf1-positive ER subdomain, and this is the first report for the identification of GTPase which regulates export of PfAK2 in *Plasmodium* species.

Figure Legends

Figure 0. Pf3D7_1020900 is a mammalian homolog of Arf1. (A) Amino acid percentage identity matrix of the six *Plasmodium* Sar/Arf familiy of GTPases and human Arf1 and Sar1. *Plasmodium* protein sequences for the Sar/Arf family of GTPases were retrieved from the PlasmoDB genome database (release 46, Nov 2019) using the Pathema

Bioinformatics Resource Center (https:// plasmodb.org/plasmo/) (Collaborative, 2001). *Plasmodium* Sar/Arf homologs were retrieved via the BLASTP algorithm using the human Arf1 and Sar1 GTPases as queries in the *P. falciparum* 3D7 database. (B) Sequence alignment of *Homo sapiens* Arf1 and Sar1 and six *Plasmodium* Sar1/Arf families of proteins. Amino acid sequences were aligned using Clustal Omega (EMBL-EBI, Welcome Genome Campus). The N-terminus myristoylation site with a glycine residue specific for the Arf family and the GTP-binding consensus boxes are indicated in blue and red boxes, respectively (Pereira-Leal and Seabra, 2000). The effector regions of the Arf/Arf-like (Arl) and Sar1 families are indicated in light blue and magenta, respectively. Note that PF3D7_1442000 and PF3D7_1316200 lack an N-terminal glycine residue. PF3D7_0920500 and PF3D7_1316200 are missing the second GTP-binding box. Two conserved residues, that are substituted to create constitutively active and inactive mutants, are indicated by black and white arrowheads, respectively. (C) Amino acid percentage identity matrix of Pf3D7_1020900 and the five human Arf1.

Table 0

Candidates for PfRab5b associated proteins.

Acc No	product	kDa	Peptide (RGF/RG)	Peptide coverage(%) (RGF/RG)
PF3D7_1310600	Rab5b GTPase	23	72/1.1	62/7.2
PF3D7_1020900	Arf1 GTPase	21	7.9/1.1	48/7.7
PF3D7_1442900	Sec7	405	11/2.3	4.6/1.2
PF3D7_1033200	ETRAMP10.2	39	5.2/1.1	17/7.6
PF3D7_0512600	Rab1b GTPase	23	4.3/1.1	23/5.5
PF3D7_0406200	Pfs16	17	3.5/0	33/0

Figure 0

A

	HsArf1	PfArf1	PF3D7_1034700	PF3D7_1442000	PF3D7_0920500	PF3D7_1316200	HsSar1a	PfSar1
HsArf1	100							
PfArf1	75	100						
PF3D7_1034700	53	51	100					
PF3D7_1442000	36	36	42	100				
PF3D7_0920500	25	24	27	23	100			
PF3D7_1316200	29	27	25	22	19	100		
HsSar1a	29	27	29	29	16	22	100	
PfSar1	33	32	32	29	20	17	52	100

B

	PfArf1	HsArf1	HsArf3	HsArf4	HsArf5	HsArf6
PfArf1	100					
HsArf1	75	100				
HsArf3	74	96	100			
HsArf4	69	80	78	100		
HsArf5	70	80	78	90	100	
HsArf6	66	68	69	64	64	100

C

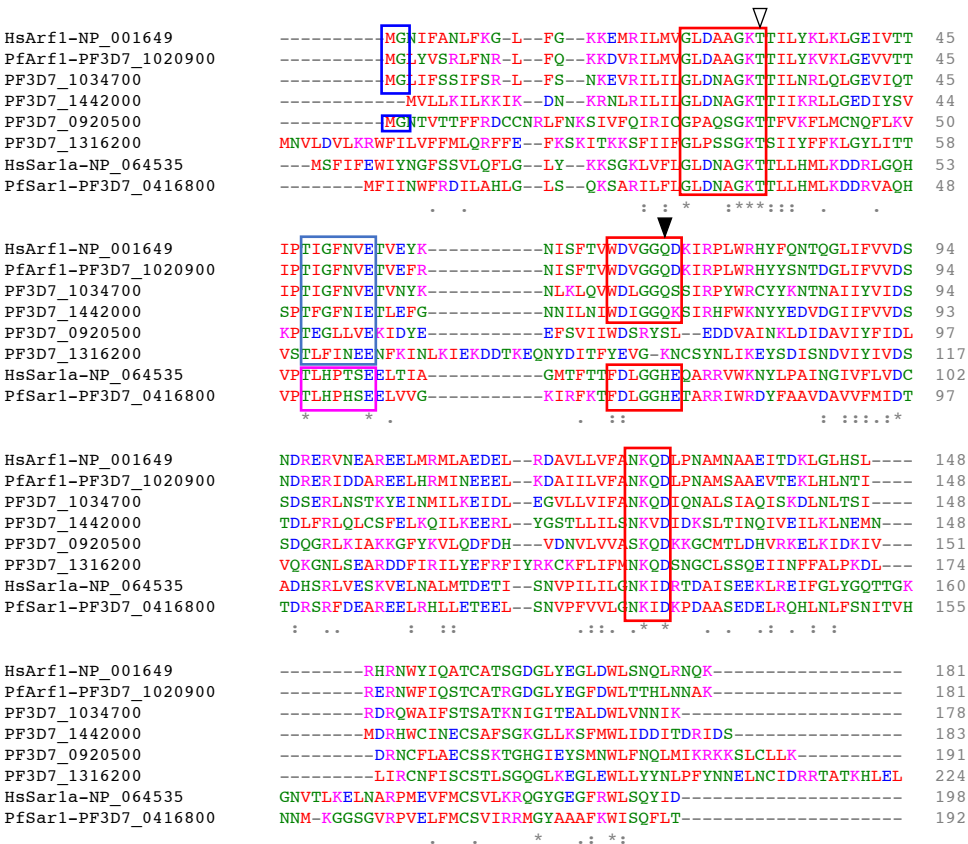

Chapter 2. Rab5b-associated Arf1 GTPase regulates export of N-myristoylated adenylate kinase 2 from the endoplasmic reticulum in *Plasmodium falciparum*

2-1 Introduction

In mammalian cell, GBF1 and BIG1, BIG2, Arf-GEFs which activate Arf GTPase, localize at cis-Golgi and trans-Golgi, TGN, respectively (Yamaji et al., 2000; Kawamoto et al., 2002; Zhao et al., 2002). Arf1 GTPase is activated by GBF1 on the cis-Golgi membrane, and recruits COPI coat proteins for the retrograde transport from the Golgi to the ER (Sager et al., 2021). Another Arf1-GTPase, which activates at the trans-Golgi and TGN membrane through BIG1 and BIG2, recruits coat proteins of clathrin-coated vesicles directed to the transport to the plasma membrane (Lefrançois and McCormick, 2007). Two isoforms of Rab1, Rab1a and Rab1b, are known in mammalian cells. Activated Rab1 GTPase involves in tethering and fusion of COPII vesicle at ERGIC and cis-Golgi by recruiting tethering protein p115 which compose tethering complex with GM130 and GRASP65 (Allan et al., 2000; Moyer et al., 2001; Appenzeller-Herzog and Hauri, 2006). Not only for anterograde transport, Rab1b GTPase also plays role in Arf1 and GBF1-mediated COPI recruitment at the cis-Golgi for retrograde transport (Alvarez et al., 2003; Monetta et al., 2007; Martinez et al., 2016).

In *P. falciparum*, colocalization of PfArf1 with the cis-Golgi marker GRASP1 was

reported previously (Thavayogarajah et al., 2015). PfRab1a and PfRab1b have been reported as two human Rab1 homologs (Quevillon et al., 2003). In contrast, PfRab1a colocalized with Rap1 and Ron4, marker of the apical organelles known as rhoptries, and regulates trafficking from the ER to the rhoptry (Morse et al., 2016), but cellular localization and function of PfRab1b has not been reported. Based on the result, PfArf1 and PfRab1b were listed as binding protein of PfRab5b which localizes at adjacent to the ER (Table 0) (Ebine et al., 2016; Hirai, 2016), I presumed PfArf1 and PfRab1b localize also close to the ER with PfRab5b not only at the Golgi. Microscopic analysis by using super-resolution microscopy was demonstrated to determine the cellular localization of PfArf1 and PfRab1b in this chapter.

As a cargo protein of PfRab5b-mediated pathway, PfAK2 which lacks signal peptide and the PEXEL-motif but possesses dual acylation at the N-terminus, has been identified based on the transport inhibition of PfAK2 by overexpression of PfRab5b (Ebine et al., 2016). In contrast, EVP1, a signal peptide and PEXEL positive protein, did not inhibit the transport to human erythrocyte by overexpression of PfRab5b, it indicates that PfRab5b-mediated pathway is independent to the conventional ER/Golgi pathway (Ebine et al., 2016). In this chapter, localizations of PfAK2 and Rifin which possesses signal peptide and the PEXEL-motif were observed under the expression of constitutively active or inactive mutant of PfArf1 or PfRab1b, to elucidate how these GTPases are involved in

the regulation of the PfRab5b-mediated pathway and the conventional ER/Golgi pathway.

2-2 Materials and Methods

2-2-1 Ethics statement

Human RBCs and plasma were obtained as donations from anonymized individuals at the Japanese Red Cross Society (No. 28J0023).

2-2-2 Strain culture and Transfection

Plasmodium falciparum line MS822 (Nakazawa et al., 2011) was cultured as described previously (Alexandre et al., 2011), and transfection was performed as described (Deitsch et al., 2001; Alexandre et al., 2011). Transfected parasites were selected with 5 nM of WR99210-HCl (a kind gift from D Jacobus) or 2.5 μg/ml of blasticidin S-HCl (BSD, Funakoshi). Transfectants were selected 2 weeks after the addition of drugs.

2-2-3 Plasmid construction

The artificial centromere plasmid PfCenV-ef1-double, whose expression was regulated under the *Plasmodium berghei* elongation factor 1 (Pbef1α) and maintained by the *P. falciparum* centromere of chromosome 5, was used to stably express PfRab5b and PfArf1 or PfRab1b (Iwanaga et al., 2012). Fusion construct of PfRab5b^{Q94L}- yellow fluorescent

protein (YFP) - destabilization domain (DD) (Armstrong and Goldberg, 2007; Watanabe et al., 2020) was inserted into the NcoI site, and PfArf1-red fluorescent protein (RFP) or RFP-PfRab1b encoding genes were ligated into the NdeI site of PfCenV-ef1-double, respectively (See Figure 9A and 9B). For expression of AK2-RFP or Rifin-RFP, fragments were inserted into the NdeI site of PfCenV-ef1-double. The AK2-RFP fragment was amplified from PfAK2-RFP/pCHD43(II)-BSD. A fragment of Rifin (PlasmoDB accession number PFA0745w) was amplified from gDNA from the *P. falciparum* 3D7 line (Walliker et al., 1987). The fusion construct consisting of PEXEL signal (1-51aa) of the Rifin-RFP-transmembrane domain (102-336aa) was described previously (Marti et al., 2004). PfArf1 and PfRab1b fragments were amplified using cDNA from the *P. falciparum* 3D7 line and the episomal plasmids expressing PfArf1-YFP-DD or DD-YFP-PfRab1b were inserted into pCHD43(II)-BSD (Ebine et al., 2016). To construct constitutively active or inactive PfArf1 (Q71L and T31N) and PfRab1b (Q67L and S22N) mutants, the PrimeSTAR Mutagenesis Basal Kit (TaKaRa Bio) was used to introduce point mutations (See Figure 9C). The former substitution at specific sites in the guanine nucleotide consensus domains of human Ras^{Q61L} impaired GTP hydrolysis activity (Haubruck and McCormick, 1991), and the latter substitution of human RasS17A altered the guanine nucleotide binding affinity for GTP to GDP (Feig and Cooper, 1988), respectively. The oligonucleotides used in this chapter are listed in Table 2.

2-2-4 Indirect immunofluorescence assay

Transgenic parasites carrying the PfRab5b, PfArf1, or PfRab1b mutant proteins fused with a DD system with artificial centromere plasmid PfCenV-ef1a-double were stabilized with 0.5 μM Shld1 for 24 h (Clontech) (Armstrong and Goldberg, 2007). Indirect immunofluorescence assay was performed as described in Chapter 1. Primary antibodies were used at the following dilutions: anti-BiP (1:100, kindly gift from Prof. Kita) and anti-ERD2 (1:100) (Elmendorf and Haldar, 1993). Alexa 488-conjugated anti-rabbit IgG (1:1,500, Molecular Probes) was used as the secondary antibody.

2-2-5 Reciprocal coimmunoprecipitation and immunoblot analysis

Transgenic parasites carrying the PfArf1-RFP, or PfArf1-RFP and PfRab5b^{Q97L}-YFP-DD with artificial centromere plasmids PfCenV-ef1a-double were cultured in 250 mL medium (5% hematocrit, 5.4% parasitemia), and collected iRBCs were permeabilized with saponin-PBS. The iRBCs were crosslinked with 2 mM DSP in 500 μL PBS for 30 min at room temperature with rotate. Samples were quenched with 50 mM Tris-HCl (pH7.5) for 15 min at room temperature with rotate, and then washed two times with 50 mM Tris-HCl (pH7.5). The sample pellets were resuspended in 500 μL lysis buffer (50 mM Tris-HCl, 150mM NaCl, Complete protease inhibitor (Roche), 1% TritonX-100, pH7.5) and homogenized by 30-times pipetting subsequently incubated on ice for 20 min.

After unbroken cells were removed by centrifugation at 2000 ×g for 5 min, the supernatants were transferred to new tubes and incubated with 20 μL Protein G Sepharose (Sigma-Aldrich) for 30 min at room temperature to reduce non-specific binding during coimmunoprecipitation. After centrifugation at 800 ×g for 5 min, the supernatant was reacted with 5 μg rabbit anti-RFP polyclonal antibody (GeneTex, GTX127897) at 4 ºC for overnight and precipitated with 30 μL Protein G Sepharose for 1 h at room temperature. The Protein G Sepharose was washed with 1 mL Lysis buffer for 3 times, and protein complexes were eluted with 40 μL of SDS sample buffer (250 mM Tris-HCl, 8% SDS, 8% 2-mercaptoethanol, 40% glycerol, 0.004% bromophenol blue, pH 6.8) at 95 ºC for 5 min. Bound proteins were eluted and loaded on 12% SDS-PAGE gels, followed by immunoblotting using mouse anti-GFP monoclonal antibody (1:100, Merck, 11814460001, clone 7.1 and 13.1) and mouse anti-RFP monoclonal antibody (1:200, Cell Biolabs AKR-021, clone RF5R), mouse anti-Hsp90 monoclonal antibody (1:500, Sigma, clone AC-16), and anti-mouse IgG conjugated HRP-linked antibody (1:10000, Cell Singling, 7076S).

2-2-6 Microscopy techniques

Images were acquired using an LSM700 or LSM780 confocal laser-scanning microscope (Zeiss, Germany). For distance measurements between PfBiP and PfArf1 or PfRab1b,

super-resolution imaging was performed using the Zeiss LSM880 with Airyscan confocal laser-scanning microscope, that is equipped with an oil-immersion 100× objective lens (alpha Plan-Apochromat 100x/1.46 Oil DIC M27 Elyra) (Zeiss, Germany). Raw data were processed using the Zeiss Zen2 software to measure fluorescent intensities. The images were analyzed using the Zeiss Zen2 software or Fiji-Image J software (Schindelin et al., 2012).

2-3 Results

2-3-1 PfArf1 and PfRab1b colocalized with PfRab5b

The intracellular colocalization of PfRab5b with PfArf1 or PfRab1b was demonstrated using double-expressing parasites. First, the constitutively active mutant PfRab5b^{Q94L} was fused with YFP and a DD (PfRab5b^{Q94L}-YFP-DD) and expressed in a Shld1 ligand-dependent manner (Armstrong and Goldberg, 2007; Ebine et al., 2016). The Q-to-L substitution in the conserved GTP binding consensus domain impairs intrinsic GTPase activity which favor formation of the active GTP-bound form to small GTPases (Der et al., 1986; Stenmark et al., 1994). As conventional Rab GTPases are modified with C-terminal geranyl-geranylation (Joberty et al., 1993), PfRab1b was fused with the N-terminal RFP (RFP-PfRab1b). In contrast, Arf1 is modified with N-terminal myristoylation (Sewell and Kahn, 1988), and PfArf1 was fused with a C-terminus RFP

fusion (PfArf1-RFP). PfRab5b^{Q94L}-YFP-DD and RFP-PfRab1b, or PfArf1-RFP were placed under the control of the Pbef1α dual promoter and the constructs were transformed into parasites (Figure 9A). Immunoblots using an anti-RFP antibody showed the 48kDa and 50kDa bands of PfArf1-RFP and RFP-PfRab1b, respectively (Figure 10). The anti-GFP antibody detected a 62kDa band corresponding to PfRab5b^{Q94L}-YFP-DD, indicating that the full length fusion constructs were expressed (Figure 10). In the early trophozoite stage, the RFP signals of PfArf1-RFP and RFP-PfRab1b were observed as juxtanuclear punctate structures, and these colocalized with the YFP fluorescence from PfRab5b^{Q94L}-YFP-DD (Figures 11A, 11B). PfRab5b^{Q94L}-YFP-DD showed good colocalization with PfArf1-RFP (average Pearson's correlation coefficient: $R = 0.51 \pm 0.088$. $n = 10$ parasites). PfRab1b-RFP showed mild colocalization with PfRab5b^{Q94L}-YFP-DD, as analysed by YFP and RFP signals (average Pearson's correlation coefficient: $R = 0.34 \pm 0.05$, $n = 10$ parasites). This result indicated that PfArf1-RFP rather than PfRab1b-RFP closely associated to PfRab5b^{Q94L}-YFP-DD (Figure 11C). The interaction of PfRab5b^{Q94L}-YFP and RFP-PfArf1 was confirmed by reciprocal coimmunoprecipitation of RFP-PfArf1 and PfRab5b^{Q94L}-YFP double-expressing parasites with anti-RFP antibody (Figure 11D). The immunoprecipitated PfRab5b^{Q94L}-YFP was recognized as 62kDa band using mouse anti-GFP antibody together with RFP-PfArf1 visualized with mouse anti-RFP antibody, while the negative control marker cytosolic protein Hsp90 was not detected in the sample. The

interaction between PfRab5b^{Q94L}-YFP and PfRab1b-RFP was not confirmed in this reciprocal coimmunoprecipitation (data not shown).

2-3-2 PfArf1 and PfRab1b were localized in different subdomains of the ER and the cis-Golgi

In an analysis conducted previously, Ebine et al. have shown that PfRab5b was localized adjacent to the ER (Ebine et al., 2016), which was labeled with the ER luminal chaperone PfBiP (Kumar et al., 1991; Kumar and Zheng, 1992). To examine the subcellular localization of PfArf1 and PfRab1b, which were colocalized with PfRab5b (Figure 11A, 11B), PfArf1-RFP or RFP-PfRab1b expressing parasites (Figure 9B) were stained with the anti-PfBiP antibody. Punctate structure signals for PfArf1-RFP and RFP-PfRab1b were closely localized with the PfBiP signals (Figure 12A). More than 70 % of PfArf1-RFP expressing parasites showed colocalization of the PfArf1-RFP and PfBiP signals (71 % ± 11 %). This proportion is higher than that of RFP-PfRab1b and PfBiP in RFP-PfRab1b expressing parasites (46 % ± 7 %, $p < 0.05$) (Figure 12B). This result was unexpected because the Arf1 and Rab1 GTPases were previously reported to be localized and targeted to the cis-Golgi in most other organisms (Stearns et al., 1990; Moyer et al., 2001). Next, PfArf1-RFP and RFP-PfRab1b expressing parasites were stained with an anti-PfERD2 antibody, which stained the *Plasmodium* homolog of the cis-Golgi

membrane protein ERD2 (Lewis and Pelham, 1990; Elmendorf and Haldar, 1993). Most of the PfArf1-RFP expressing parasites did not show colocalization of the PfArf1-RFP and PfERD2 signals (32 % ± 9 %) (Figures 12C, 12D). The ratio of PfRab1b colocalization with PfERD2 was increased to 59 % ± 3 % in PfRab1b-RFP expressing parasites ($p < 0.05$) (Figures 12C and 12D). These results indicate that both PfArf1 and PfRab1b simultaneously localize to the ER and cis-Golgi in this organism; however, the subcellular localization fraction differed between PfArf1 and PfRab1b, as most of the PfArf1 was localized to the proximal region of the ER, and half of PfRab1b was individually localized to the ER and the cis-Golgi.

Detailed analysis using super-resolution microscopy enabled the identification of the distinct subcellular localization of PfArf1 and PfRab1b on the ER, and whether both GTPases localize to the same subdomain or reside in distinct regions. The immunostained slides were processed with a super-resolution microscope LSM880 with Airyscan and processed with Zeiss Zen2 software, which provides a lateral resolution of 140 nm, to analyze the precise cellular locations of the proteins. Peak signal intensities of the most proximal staining between PfBiP and PfArf1-RFP (Figure 13A) or PfRab1b (Figure 13B) were calculated. The average distance from PfBiP was closer to PfArf1-RFP than to RFP-PfRab1 (PfArf1-RFP: 0.33 ± 0.08 μm vs. RFP-PfRab1 0.45 ± 0.11 μm, $p < 0.001$) (Figure 13C). These data indicate the presence of compartmentalization in the ER or ER adjacent

novel membrane structures, and PfArf1 showed significant localization close to the PfBiP-positive ER rather than PfRab1b.

2-3-3 PfArf1 and PfRab1b are involved in the transport of the PEXEL-positive transmembrane protein Rifin

Blood stage parasites export several proteins into the host erythrocyte cytosol and the PV (Sargeant et al., 2006; van Ooij et al., 2008). The PEXEL sequence is a five-residue motif in the downstream N-terminal signal peptide, and it has been detected in many exported proteins (Hiller et al., 2004; Marti et al., 2004). PEXEL-positive proteins have been suggested to pass through the classical ER/Golgi pathway (Akompong et al., 2002). However, the presence of several PNEPs indicates the existence of an alternative export pathway (Möskes et al., 2004; Thavayogarajah et al., 2015). It has been shown previously that overexpression of PfRab5b did not disrupt the export of the PEXEL-positive transmembrane protein EVP1 to the iRBC cytosol (Ebine et al., 2016). To examine whether PfArf1 and PfRab1b are involved in trafficking of PEXEL-positive export proteins, I chose a Rifin variant PFA0745w, whose fusion construct with YFP was secreted into the erythrocyte cytosol (Marti et al., 2004). The N-terminal PEXEL domain and the C-terminal transmembrane region were fused with RFP (Rifin-RFP) and co-expressed with the PfArf1 and PfRab1b mutant constructs, whose expression was driven

by the Shld1 ligand (Figure 9C). No growth defect was detected in these transformants (Figure 14). In parasites expressing the PfArf1^{WT}-YFP-DD and active mutant PfArf1^{Q71L}-YFP-DD constructs, Rifin-RFP signals were detected in the iRBC plasma membrane and at the parasite periphery (PfArf1^{WT}: 91 % ± 4 %, PfArf1^{Q71L}: 88 % ± 6 %) (Figures 15A and 15B). In contrast, the export of Rifin-RFP reduced the inactive PfArf1^{T31N}-YFP-DD expressing parasites (53 % ± 12 %) (Figures 15A and 15B), suggesting that PfArf1 is involved in PEXEL-positive Rifin transport. Similarly, the expression of wild-type DD-YFP-PfRab1b and the active mutant DD-YFP-PfRab1b^{Q67L} did not show differences for the export of Rifin-RFP (PfRab1b^{WT}: 89 % ± 2 %, PfRab1b^{Q67L}: 90 % ± 10 %), whereas the expression of the inactive mutant DD-YFP-PfRab1b^{S22N} reduced the export activity (39 % ± 9 %) (Figures 15C and 15D).

2-3-4 PfArf1, but not PfRab1b, regulates the export of N-acylated adenylate kinase 2 to the PVM

Adenylate kinase 2 (PfAK2) is an N-terminal myristoylated and palmitoylated protein, which lacks the signal peptide and a transmembrane domain. It localizes to the parasite plasma membrane face to the PV (Thavayogarajah et al., 2015; Ebine et al., 2016), suggesting that PfAK2 was not exported through the classical ER/Golgi-dependent pathway. Ebine et al. have previously reported that overexpression of PfRab5b-YFP-DD

disrupted the transport of PfAK2-RFP to the PVM (Ebine et al., 2016). Overexpression of PfRab5b-YFP-DD altered the peripheral staining of PfAK2-RFP in the parasite cytoplasmic staining pattern, indicating that PfRab5b might be involved in the transport of PfAK2 (Ebine et al., 2016). Therefore, I examined whether the overexpression of PfArf1 perturbs the transport of PfAK2-RFP to the PVM. Parasites that double-expressed PfAK2-RFP and PfArf1WT, or the constitutively active PfArf1^{Q71L} or inactive PfArf1^{T31N} mutants (Figure 16A), whose expression is driven by the Shld1 ligand were established (Figure 9C). The PfArf1^{Q71L} and PfArf1^{T31N} mutants are corresponding to human Arf1^{Q71L} and Arf1^{T31N}, respectively (Dascher and Balch, 1994; Teal et al., 1994). In the PfArf1^{WT}-YFP-DD expressing parasite, all PfAK2-RFP signals were localized at the parasite periphery, indicating a typical PVM staining pattern (Figure 16A). In contrast, the active mutant PfArf1^{Q71L}-YFP-DD expressing parasites reduced PfAK2-RFP targeting to the PVM (38 % ± 6.7 %). Several parasites showed a faint RFP signal and a punctate RFP signal within the parasite cytoplasm (faint: 35 % ± 7.1 %, punctate: 27 % ± 7.7 %, respectively) (Figures 16A and 16B). In the inactive PfArf1^{T31N}-YFP-DD expressing parasite, the export of PfAK2-RFP was reduced to 58 % ± 6.8 %, and further, 13 % ± 7.2 % and 29 % ± 11 % of the parasites showed a faint RFP signal and a punctate pattern in the cytoplasm, respectively (Figures 16A and 16B). The faint signal of PfAK2-RFP was more abundant in PfArf1^{Q71L}-YFP-DD than in PfArf1^{T31N}-YFP-DD ($p < 0.05$). These

results indicate that PfArf1 is directly involved in the correct export of PfAK2 to the PVM. The specific role of PfArf1 in the transport of PfAK2 was highlighted by the co-expression of PfRab1b mutants (Figures 16C). In the co-expression with the wild-type DD-YFP-PfRab1b, active DD-YFP-PfRab1b^{Q67L}, or the inactive DD-YFP-PfRab1b^{S22N} constructs, which corresponds human Rab1b^{Q67L} and Rab1b^{S22N}, respectively (Tisdale et al., 1992), the transport of PfAK2-RFP was not inhibited and all parasites showed a peripheral pattern for their expression (PfRab1b^{WT}: 99 % ± 2 %, PfRab1b^{Q67L}: 96 % ± 4 %, PfRab1b^{S22N}: 94 % ± 3 %) (Figures 16C and 16D). These results suggest that PfArf1 is extensively involved in the transport of the N-acylated protein PfAK2 to the PVM.

2-4 Discussion

2-4-1 PfArf1 exports the N-myristoylated protein PfAK2 to the PVM

The regulatory mechanisms underlying the trafficking of acylated proteins are not clearly understood in *Plasmodium* species and other organisms. Dual acylated proteins are first myristoylated at the ER membrane by N-myristoyl transferase after palmitoylation by a palmitoyltransferase, and the acylated proteins are then trafficked to the apical organelle and parasite plasma membrane surface (Cabrera et al., 2012). For other proteins, such as the *Plasmodium falciparum* calcium-dependent protein kinase 1 (PfCDPK1) and the Drosophila transgultaminase A (TG-A), the dual acylated proteins are packed into

multivesicular bodies and are subsequently exported to the apical organelle or extracellular space via the unconventional ER-Golgi-independent pathway (Möskes et al., 2004; Shibata et al., 2017). Ebine et al. have previously shown that the transport of N-myristoyl PfAK2 to the PVM was inhibited by the overexpression of PfRab5b, and that PfAK2 accumulated in the punctate structure within the parasite cytoplasm together with PfRab5b, indicating that PfRab5b and PfAK2 were included in the internal vesicle of the multivesicular body and were then transported to the PVM (Ebine et al., 2016). In this study, I have shown that PfArf1, but not PfRab1b, is involved in the regulation of PfAK2 (Figures 16A and 16C). My results indicated that the expression of active or inactive PfArf1 mutants inhibited PfAK2 transport to PVM (Figure 16A), whereas the expression of active or inactive PfRab1b mutants had no effect (Figure 16C). These results suggest that GTP hydrolysis by PfArf1 is required for proper PfAK2 recognition and further transport. For mammalian Arf1, it has been biochemically demonstrated that GTP hydrolysis by human Arf1 promotes the selective cargo selection from the Golgi membrane, and the concentration of cargo proteins into the COPI-coated vesicles (Lanoix et al., 1999). This observation indicated that the role of GTP hydrolysis in cargo selection is similar between PfArf1 and the human Arf1.

2-4-2 Presence of subdomains near the ER and the sequential roles of PfArf1 and PfRab1b in cargo selection

Both PfArf1 and PfRab1b are localized close to the ER as punctate structures in the early erythrocytic stage (Figure 11A and 11B). The punctate structure near the ER was observed in other proteins, such as the COPII coat components PfSec13 and PfSec24 (Lee et al., 2008; Struck et al., 2008) and in another PfRab1 isotype PfRab1a (Morse et al., 2016). Previously, Ebine et al. have shown that PfRab5b did not colocalize with the COPII component PfSec13 (Struck et al., 2008; Ebine et al., 2016), suggesting that PfArf1 and PfRab1b might be localized in different domains from the COPII vesicle budding site, the ERES. In this study, the results indicate that the PfArf1 signal was not completely consistent with that for PfRab1b and was localized to different membrane subdomains around the ER (Figure 13). These findings suggest that the previously reported COPII component, PfArf1, and PfRab1b might be localized to an independent subdomain and may have different roles in the transport of cargo proteins and cargo selection from the ER. PfRab1b was involved in the transport of the PEXEL-positive export protein, Rifin, and the expression of the inactive PfRab1b mutant showed decreased activity of Rifin export to erythrocyte cytosol (Figure 15C and 15D). In contrast, the expression of the active PfRab1b mutant did not inhibit Rifin export, indicating that the GTP-bound state of PfRab1b may be necessary for the proper functioning of PfRab1b. A similar

observation was reported in mammalian Rab5 during endosome fusion, where it was demonstrated that the GTP-bound mutant form showed the same effect as the wild-type Rab (Barbieri et al., 1996).

Interestingly, the export of Rifin was also decreased by the expression of inactive mutants of PfArf1, but not the active mutants and the wild-type PfArf1 (Figures 15A and 15B). This result suggests that the GTP-bound state of PfArf1 is necessary for the export of Rifin, or for the correct activity of PfRab1b. Although not included in this study, it is notable that a Sec7 domain containing protein was listed as a candidate for the PfRab5b binding protein using mass analysis (Table 0)(Hirai, 2016). The 200 amino acid residue Sec7 domain is conserved among eukaryote and has the guanine nucleotide exchange activity towards Arf (Arf GEF) (Cherfils et al., 1998). In other organisms, Sec7 is involved in the "Rab cascade": activated GTPase triggers the recruitment of GEF for the downstream GTPase, and thus a series of GTPase activations is feasible (Barr, 2013). For example, in *Saccharomyces cerevisiae*, Ypt1 (in yeast Rab1) and the Arf-like GTPase Arl1 recruit Sec7 to the Golgi membrane, and subsequently Arf1 is activated by the GEF activity of membrane-localized Sec7, following the stimulation of Ypt31 (yeast Rab11) on the trans-Golgi membrane for cargo sorting to secretory vesicles (McDonold and Fromme, 2014). Thus, I generated a sequential hypothetical model of PfArf1 and PfRab1b adjacent to the ER that is presented in Figure 17. Membrane-localized PfRab5b may

recruit PfSec7 to activate PfArf1 in the adjacent ER subdomain, where the N-myristoylated protein PfAK2 is selected and packed into the pathway destined for the PVM. This is based on the finding that colocalization of the active mutant of PfRab5b and PfArf1 (Figure 11A), and wild-type PfArf1 is necessary for the export of PfAK2 (Figure 16A). It has been shown that *Plasmodium* PfArf1 possesses GTPase activity in vitro (Stafford et al., 1996) and that PfSec7 accelerated the nucleotide exchange activity against PfArf1 (Baumgartner et al., 2001). Thus, the PfArf1 may colocalize with PfSec7 adjacent to the ER. The role of PfSec7 in intracellular traffic remains elusive, and further studies are needed to unravel the regulation of PfAK2 transport together with PfArf1. Subsequently, the PfArf1 positive membrane matures and recruits PfRab1b at the membrane. This model is based on my results that indicate that PfRab1b localizes to the different subdomains of PfArf1 that are adjacent to the ER (Figures 11B and 13), and that the sequential recruitment of different GTPases to the membrane occurs via Sec7 (McDonold and Fromme, 2014). The Rab1 positive membrane subdomain near the ER is found in mammalian tubulovesicular membrane clusters of the ER-Golgi intermediate compartment (ERGIC) (Appenzeller-Herzog and Hauri, 2006). ERGIC clusters lie close to the COPII-positive ERES. Transport from the ER to the ERGIC is controlled by COPII coat vesicles, and Rab1 is involved in membrane tethering at the ERGIC in anterograde transport (Allan et al., 2000). Sorting in the ERGIC involves another protein coat of COPI

and the Arf family (Goldberg, 2000). Thus, ERGIC is a sorting and recycling platform for the transport between the ER and Golgi in mammalian cells. In *Plasmodium*, the PfRab1b-positive compartment was involved in the export of the PEXEL-positive protein Rifin (Figure 15) and this suggests the existence of a novel sorting compartment for PEXEL-positive cargo proteins. The model shown in Figure 17 indicates the segregation of the subdomain for sorting of different cargo proteins. Conversely, the expression of active and inactive PfRab1b mutants did not affect the export of PfAK2 (Figure 16).

2-4-3 Transport to the Golgi and the presence of a few parts of PfArf1 on the PfERD2 positive Golgi membrane

In most mammalian secretory cells, electron microscopy has revealed the presence of ribosome-coated rough ER and partly smooth surfaced structures in the vicinity of the Golgi complex (Saraste and Kuismanen, 1992). Golgi is displayed as stacks of flattened cisternae, which are often laterally linked into a ribbon-like structure (Zhang and Wang, 2016). In contrast, the ER and Golgi of malarial parasites are not well characterized and are reported to be loosely associated vesicles (Aikawa, 1971). To overcome the difficulty in the visualization of ER and the Golgi, I used super-resolution fluorescence microscopy (Figure 13) and quantified the number of colocalized parasites (Figures 12, 13, 15,16). In this study, about 70 % of parasites showed colocalization of PfArf1 and the ER marker

PfBiP, and 30 % showed colocalization with the cis-Golgi marker PfERD2 (Figure 12). These results may explain the following two possibilities. One; PfArf1 is a Golgi resident which is involved in retrograde trafficking from the Golgi. This model is based on reports from mammalian and yeast models, where Arf1 is involved in different steps of cargo sorting together with specific effector or Sec7 containing proteins such as retrograde traffic from the cis-Golgi to the ER, or the secretory pathway from the trans-Golgi (Donaldson and Jackson, 2011). As it is not yet characterized, the Golgi resident PfArf1 may be involved in retrograde trafficking to the ER because the homolog of ERD2 is present and localized to the Golgi in *Plasmodium* (Elmendorf and Haldar, 1993). ERD2 retrieves the conserved C-terminal tetrapeptide sequence HDEL-containing ER luminal proteins from the cis-Golgi in yeast and mammalian cells (Hsu et al., 1992; Townsley et al., 1994). A second possibility is the presence of the Golgi subdomain in *Plasmodium* species. The *Plasmodium* ERD2 was previously reported to colocalize with the Golgi re-assembly stacking protein (GRASP) (Struck et al., 2005), and PfArf1 was shown to be colocalized with GRASP in the early trophozoite stage (Thavayogarajah et al., 2015). Therefore, it appears that PfArf1, GRASP, and PfERD2 are colocalized in the same Golgi membrane. However, mammalian GRASP55 is present in the medial/trans-cisternae of Golgi stacks as shown by cryo-immunoelectron microscopy (Langreth et al., 1978). Thus, this may be the reason for the Golgi-stacked protein GRASP and HDEL-receptor ERD2

to colocalize in the same Golgi subdomain in *Plasmodium*.

2-5 Figure Legends

Figure 9. Schematic structure of the constructs used in this study. (A) The artificial centromere plasmid PfCenV-ef1-double was inserted two fragments in NcoI and NdeI sites, whose expression is regulated under the *Plasmodium berghei* elongation factor 1 (Pbef1α). In NcoI site, PfRab5b^{Q94L}-YFP-DD was inserted and RFP- PfArf1 (upper) or PfRab1b-RFP (lower) was inserted in the NdeI site. (B) RFP-PfArf1 (upper) or PfRab1b-RFP (lower) was inserted in the NdeI site of the centromere plasmid for the single expression. (C) To double express GTPase (PfArf1 and PfRab1b) and cargo proteins (PfAK2 and Rifin), PfArf1-YFP-DD (upper, left) or DD-YFP-PfRab1b (lower, left) fragment was inserted into episomal plasmid pCHD43(II), whose hDHFR cassette was replaced with a blasticidin S-resistance cassette (Ebine et al., 2016). Cargo proteins, PfAK2-RFP (upper, right) or Rifin-RFP (lower, right) fusion constructs, were inserted into PfCenV-ef1-double of NdeI site. Each GTPase and cargo protein construct was transfected into the parasite, and simultaneously selected with WR99210 and blasticidin S. proCRT, the constitutive *P. falciparum* chloroquine resistance transporter promoter: PbDT, *Plasmodium berghei* dihydrofolate reductase terminator proPfCAM, *P. falciparum* calmodulin promoter, hDHFR, human dihydrofolate reductase: PfHRPII, *P. falciparum*

histidine-rich protein II termiator: rep20, element to improve episomal segregation at mitosis: PfCenV, the centromere of chromosome 5: BSD, blasticidin S.

Figure 10. Immunoblots showing the expression of full length of PfArf1-RFP, and RFP-PfRab1b. Parasite lysates expressing PfRab5b^{Q94L}-YFP-DD and Arf1-RFP or RFP-PfRab1b were subjected to immunoblot analysis using anti- RFP and anti-GFP antibodies. Anti-Hsp90 antibody was used as a loading control. Mock is the non-transformant parasite.

Figure 11. Association of PfRab5b and PfArf1 GTPases rather than PfRab1b in adjacent to the nucleus. Transformant parasites carrying the PfArf1-RFP (A, red) or PfRab1b-RFP (B, red) constructs with PfRab5b^{Q94L}-YFP-DD (green) under the dual Pfef1α promoter were stabilized with Shld1, and were then used in the immunofluorescence assay. The fluorescence of RFP and YFP was captured. Arrowheads indicate the colocalization of PfArf1 and PfRab1b with PfRab5b^{Q94L}. The nuclei were stained with DAPI (blue). Representative images showing mononuclear early trophozoite (upper), two nuclear late trophozoite (middle), and multinucleated early schizont (lower) stages are shown. White arrowheads indicate the colocalization of PfRab5b^{Q94L}-YFP-DD and PfArf1-RFP or PfRab1b-RFP. The bars indicate 2 μm. (C) Pearson's correlation coefficient between

PfRab5b^{Q94L}-YFP-DD and PfArf1-RFP or RFP-PfRab1b. The fluorescence intensities of the merged YFP and RFP signals were analyzed using Fiji-Image J software to generate Pearson correlation coefficients. The scatter plot represents Pearson correlation coefficients values from ten independent parasites, which are obtained from three independent transfectants. The statistical significance was determined using Student's *t*-test. (D) Reciprocal immuoprecipitation experiments of PfArf1-RFP via interaction with PfRab5b^{Q94L}-YFP-DD. PfRab5b^{Q94L}-YFP-DD and PfArf1-RFP double- expressing parasites were crosslinked with DSP as described in Materials and Methods, and immunoprecipitated with rabbit anti-RFP antibody (IP: +). Immunoprecipitated PfArf-RFP (a white arrowhead) and PfRab5b^{Q94L}-YFP-DD (a black arrowhead) was visualized with mouse anti-RFP or anti-GFP antibodies, respectively. In the absence of rabbit anti-RFP antibody during immnoprecipitation (IP: －), neither PfArf-RFP nor PfRab5b^{Q94L}-YFP-DD was detected. Anti-Hsp90 antibody was used as a negative control. Two 50 kDa bands in pull down fraction (an asterisk) were non-specific recognition of secondary antibody against anti- rabbit IgG.

Figure 12. Localization of PfArf1 and PfRab1b in juxtaposition to the ER and the cis-Golgi. (A) Synchronized parasites, expressing PfArf1-RFP (upper, red) or RFP- PfRab1b (lower, red), were fixed at early trophozoite stage and subjected to the indirect

immunofluorescence analysis with anti-PfBiP antibody (green) and DAPI (blue). The fluorescence of PfArf1-RFP and RFP-PfRab1b is shown. PfBiP was stained with an anti-PfBiP antibody. Both PfArf1-RFP and RFP-PfRab1b localized adjacent to the PfBiP signal (arrowheads). (B) Rate of colocalization of PfArf1-RFP and RFP-PfRab1b with PfBiP. The number of parasites that showed colocalization of the RFP and PfBiP signals was counted in 20–30 trophozoites from three independent experiments. Error bars indicate the standard deviations of three replicates. A test for statistical significance was performed using the Student's *t*-test. (C) Indirect immunofluorescence analysis of the localization of PfArf1-RFP (upper, red), RFP- PfRab1b (lower, red), the cis-Golgi-marker PfERD2 (green), and DAPI (blue). The fluorescence from RFP-PfRab1b colocalized with the PfERD2 signal (arrowhead), but not with PfArf1-RFP. The bars indicate 2 μm. (D) Rate of colocalization of PfArf1-RFP and RFP-PfRab1b with PfERD2. The number of parasites that showed colocalization of the RFP and PfERD2 signals was counted in 20–30 trophozoites from three independent experiments. A test for statistical significance was performed using the Student's *t*-test.

Figure 13. Super-resolution imaging showing the fine differences between PfBiP and PfArf1 or PfRab1b. Synchronized parasites, expressing PfArf1-RFP (A, red) or RFP-PfRab1 (B, red), were sampled at early trophozoite stage and fixed and subjected indirect

immunofluorescence analysis with the anti-PfBiP antibody (green) and DAPI (blue). Fluorescence intensities along the bold white lines are indicated in the graphs on the right. The fluorescence intensity was calculated as the percentage of the highest signal intensities. Black arrowheads depict the peaks of RFP and PfBiP intensities. The bars indicate 2 μm. (C) The smallest calculated distances between (A, B) in 15 independent parasites were plotted, and the average (bold bars) and standard deviation (thin bars) are indicated. A test for statistical significance was evaluated using the Student's *t*-test.

Figure 14. Expressions of PfArf1 or PfRab1b mutants showed no effect on parasites growth. The population doubling time of non-transformant MS822 line, PfArf1 and PfRab1b mutants were measured for 2 days cultivation from three independent assays. The average (bar graph) and the standard deviation (thin bar) are indicated. Mock was cultured without drugs and PfArf1, PfRab1b mutants were cultured with BSD. Except from MS822 line, transformed parasites were cultured in the presence of 2.5 μg/ml of BSD and the expressions of PfArf1 and PfRab1b mutants were stabilized by 0.5 μM Shld1. A statistical significance was evaluated using Student's *t*-test.

Figure 15. PfArf1 and PfRab1b regulated the export of PEXEL-positive Rifin to the erythrocyte cytoplasm. Parasites expressing Rifin-RFP and PfArf1-YFP-DD (A, B) or

DD-YFP-PfRab1b (C, D) were examined via the immunofluorescence assay. Fluorescence signals from RFP (red), YFP (green), and DAPI (blue) are shown. Wild-type PfArf1 or PfRab1b (upper panels), active mutant PfArf1^{Q71L} or PfRab1b^{Q67L} (middle panels), and the inactive mutant PfArf1^{T31N} or PfRab1b^{S22N} (lower panels) are shown. White dotted lines indicate the parasite plasma membrane. The arrowheads indicate dot-like exported Rifin-RFP signals. The bars indicate 2 μm. The rate of parasites that showed a Rifin-RFP signal was detected in the erythrocyte cytoplasm in PfArf1-RFP (B) and RFP-PfRab1b (D) expressing cells are shown in graphs. Thirty individual early trophozoites and early schizonts were counted from three independent experiments. Infected RBCs, recognized by the DAPI and YFP signals under the microscope, were imaged by the laser microcopy, and then analyzed for the localization of RFP and whether Rifin-RFP was exported to the iRBC. The statistical significance was determined using the Student's *t*-test.

Figure 16. The specific role of PfArf1 in the transport of N-acylated PfAK2 to the PVM. Parasites expressing PfAK2-RFP and PfArf1-YFP-DD (A, B) or DD-YFP-PfRab1b (C, D) were examined using the immunofluorescence assay. Fluorescence signals from RFP (red), YFP (green), and DAPI (blue) are shown. Wild-type PfArf1 or PfRab1b (upper panels), the active mutant PfArf1^{Q71L} or PfRab1b^{Q67L} (middle panels), and the inactive

mutant PfArf1^{T31N} or PfRab1b^{S22N} (lower panels) are shown. Representative images for PfAK2-RFP are shown and are divided into three patterns: peripheral PVM staining (PVM), faint signal (faint), and dot-like punctate signal within the parasites (punctate). The bars indicate 2 μm. The parasites that showed a signal for PfAK2-RFP were classified into three patterns based on the PfArf1-RFP expressing cells (B) and then shown in bar graph. The rate of parasites showing peripheral staining for PfAK2-RFP in RFP-PfRab1b expressing cells (D). Thirty individual early trophozoites and early schizonts were counted from three independent experiments. Infected RBCs, recognized by the DAPI and YFP signals under the microscope, were imaged by the laser microcopy, and then analyzed for the localization of RFP signal as PV, faint, and punctate. The statistical significance was determined using the Student's *t*-test.

Figure 17. A proposed model for the two pathways regulated by PfArf1 and PfRab1b. PfRab5b (blue circle) recruited PfArf1 (red circle) probably through the binding to PfArf1 activating protein (light grey ellipse) on the ER membrane (Figure 12). Membrane targeted PfArf1 selected the N-acylated AK2 and sorted into the pathway for the PV (Figure 16). According to the partial involvement of PfArf1-positive membrane for the selection of PEXEL-positive Rifin (Figure 15), and PfRab1b (yellow circle) localized to distant membrane from the ER (Figure 14), PfArf1-positive membrane might be matured

into PfRab1b-positive compartment. PfRab1b- positive compartment selects and further transports the PEXEL-positive Rifin to the RBC surface. ER, endoplasmic reticulum; ERES, endoplasmic reticulum exit site; PV, parasitophorous vacuole; RBC, red blood cell.

PfAK2

Figure 9

A

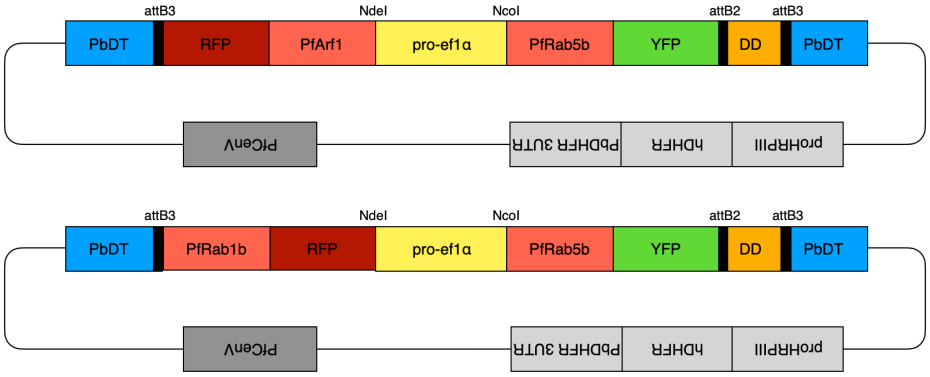
attB3
NdeI
NcoI
attB2
attB3
PbDT
RFP
PfArf1
pro-ef1α
PfRab5b
YFP
DD
PbDT
PfCenV
PbDHFR 3UTR
hDHFR
proHRPIII
attB3
NdeI
NcoI
attB2
attB3
PbDT
PfRab1b
RFP
pro-ef1α
PfRab5b
YFP
DD
PbDT
PfCenV
PbDHFR 3UTR
hDHFR
proHRPIII

B

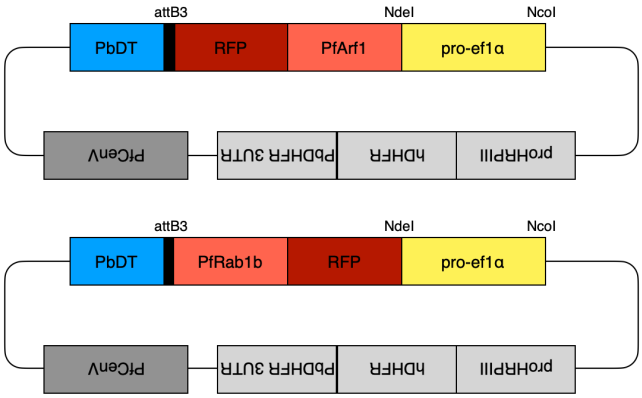
attB3
NdeI
NcoI
PbDT
RFP
PfArf1
pro-ef1α
PfCenV
PbDHFR 3UTR
hDHFR
proHRPIII
attB3
NdeI
NcoI
PbDT
PfRab1b
RFP
pro-ef1α
PfCenV
PbDHFR 3UTR
hDHFR
proHRPIII

C

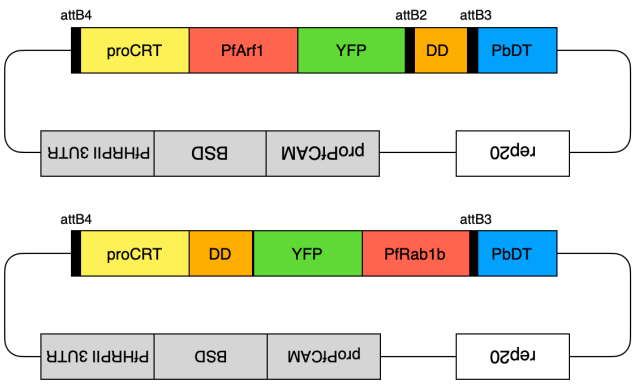
attB4
attB2
attB3
proCRT
PfArf1
YFP
DD
PbDT
PfHRPII 3UTR
BSD
proPfCAM
rep20
attB4
attB3
proCRT
DD
YFP
PfRab1b
PbDT
PfHRPII 3UTR
BSD
proPfCAM
rep20

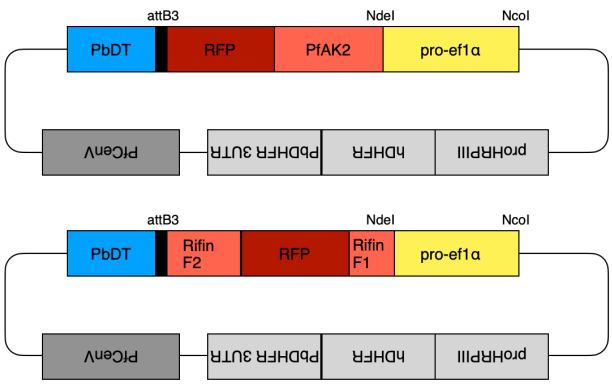
attB3
NdeI
NcoI
PbDT
RFP
PfAK2
pro-ef1α
PfCenV
PbDHFR 3UTR
hDHFR
proHRPIII
attB3
NdeI
NcoI
PbDT
Rifin F2
RFP
Rifin F1
pro-ef1α
PfCenV
PbDHFR 3UTR
hDHFR
proHRPIII

Figure 10

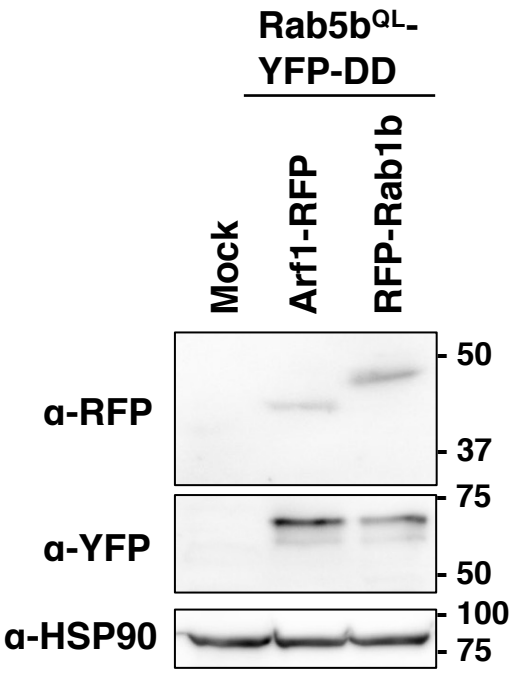
Rab5b^QL-YFP-DD
Mock
Arf1-RFP
RFP-Rab1b
α-RFP
α-YFP
α-HSP90
50
37
75
50
100
75

Figure 11

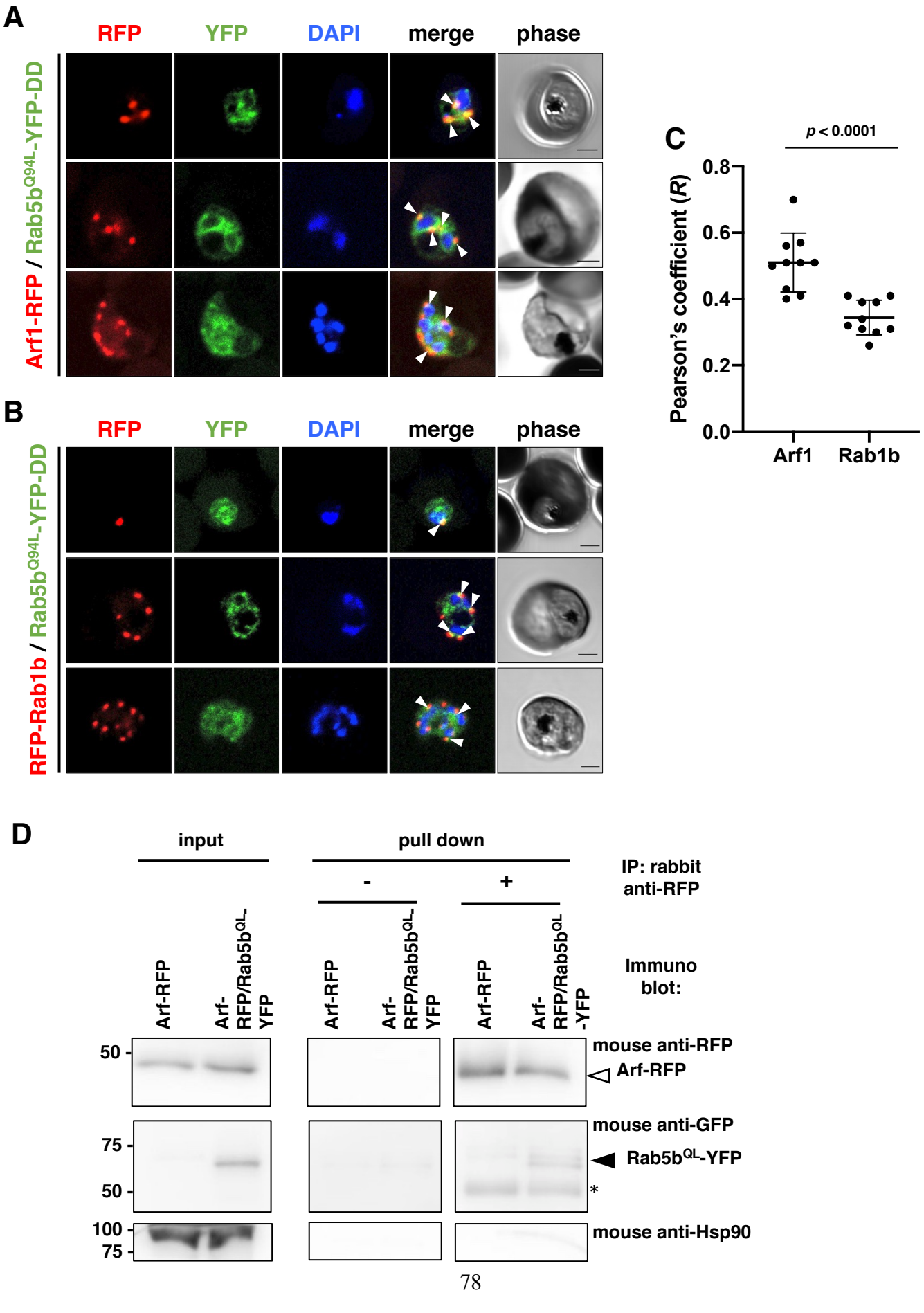
A
RFP
YFP
DAPI
merge
phase
Arf1-RFP / Rab5b^{Q94L}-YFP-DD
B
RFP
YFP
DAPI
merge
phase
RFP-Rab1b / Rab5b^{Q94L}-YFP-DD
C
$p < 0.0001$
Pearson's coefficient (R)
0.8
0.6
0.4
0.2
0.0
Arf1
Rab1b
D
input
pull down
IP: rabbit anti-RFP
-
+
Arf-RFP
Arf-RFP/Rab5b^{QL}-YFP
Arf-RFP
Arf-RFP/Rab5b^{QL}-YFP
Arf-RFP
Arf-RFP/Rab5b^{QL}-YFP
Immuno blot:
50
mouse anti-RFP
Arf-RFP
75
50
mouse anti-GFP
Rab5b^{QL}-YFP
*
100
75
mouse anti-Hsp90

Figure 12

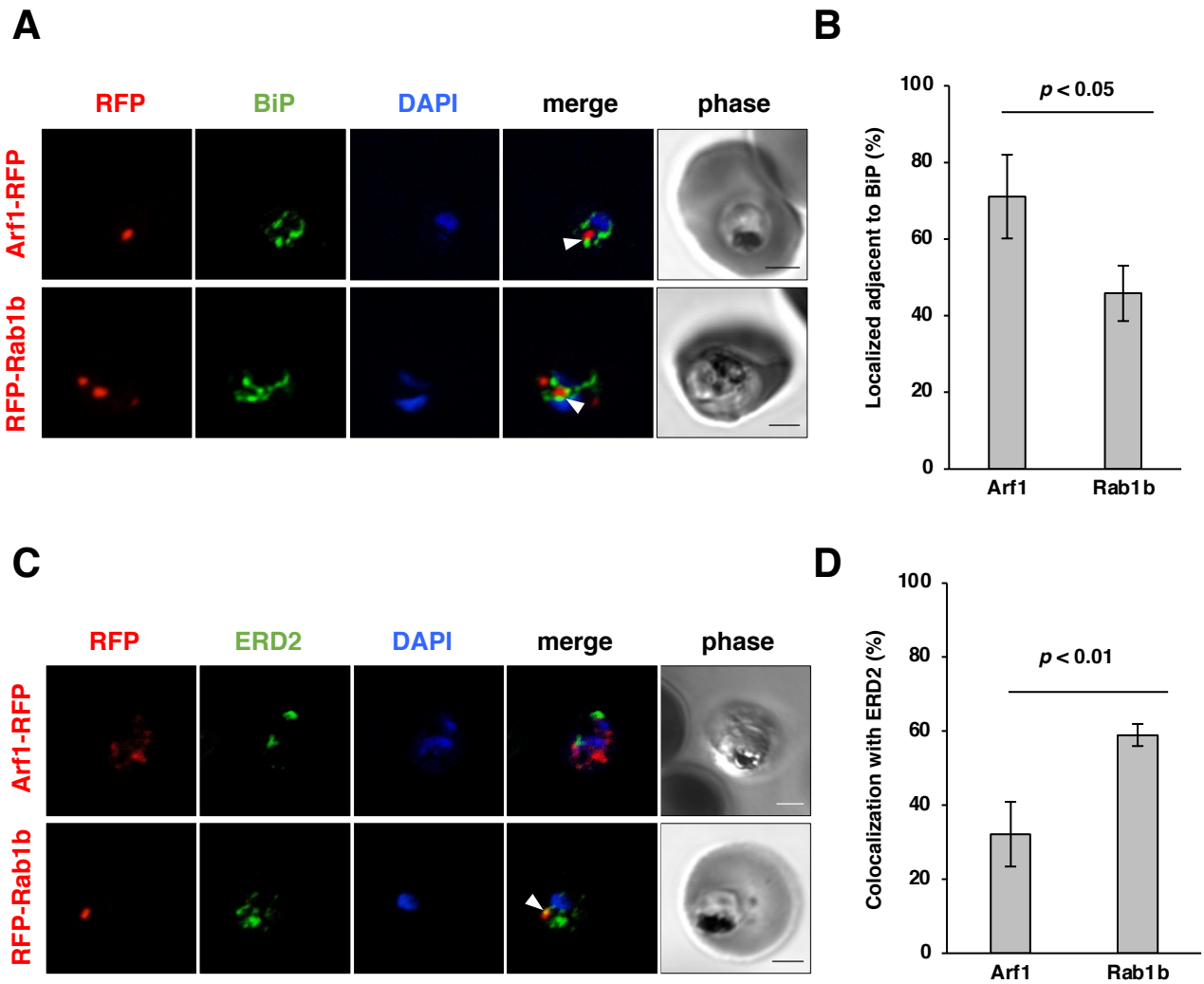
A
RFP
BiP
DAPI
merge
phase
Arf1-RFP
RFP-Rab1b
B
p < 0.05
Localized adjacent to BiP (%)
100
80
60
40
20
0
Arf1
Rab1b
C
RFP
ERD2
DAPI
merge
phase
Arf1-RFP
RFP-Rab1b
D
p < 0.01
Colocalization with ERD2 (%)
100
80
60
40
20
0
Arf1
Rab1b

Figure 13

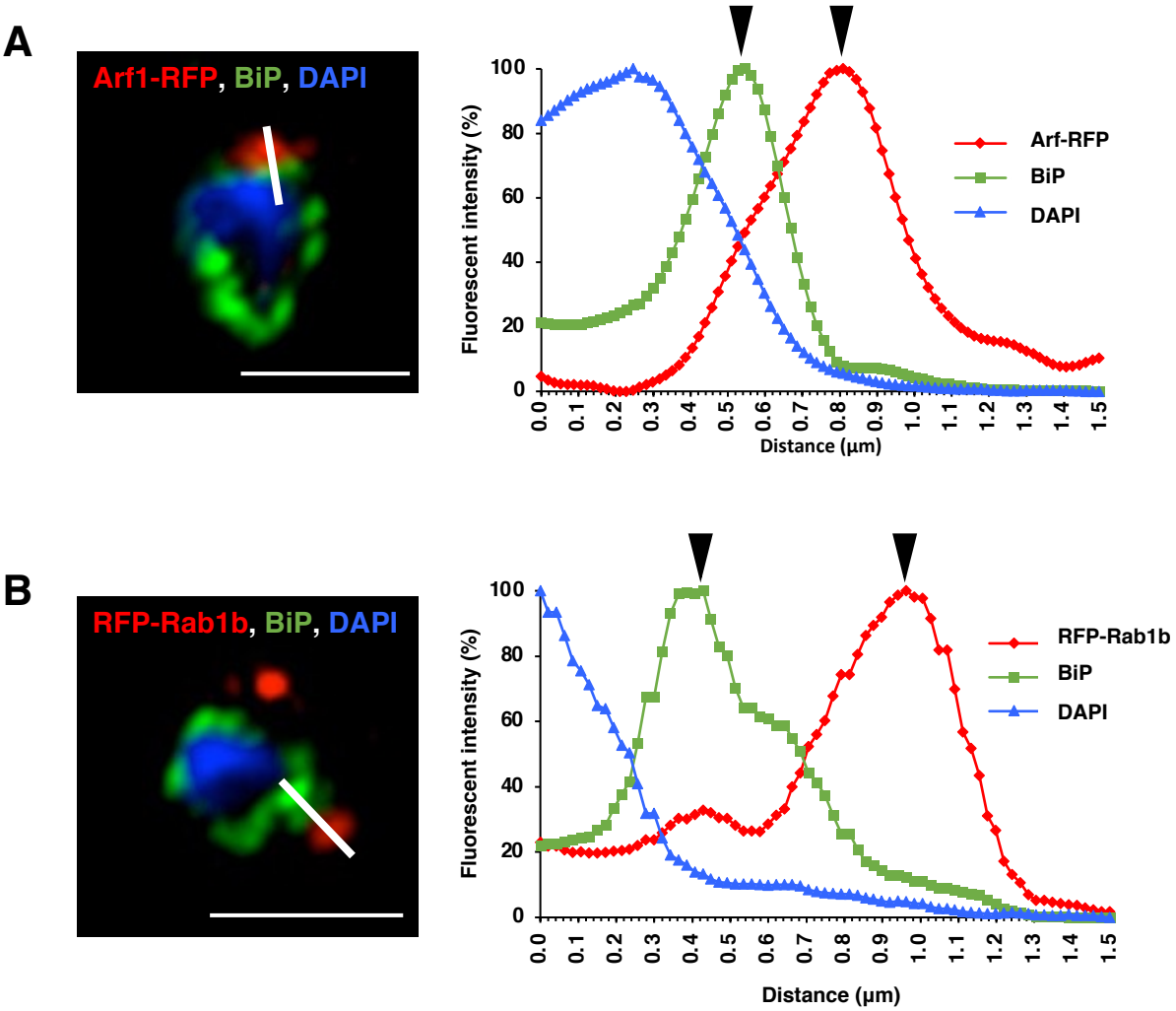
A
Arf1-RFP, BiP, DAPI
Fluorescent intensity (%)
Distance (μm)
Arf-RFP
BiP
DAPI
B
RFP-Rab1b, BiP, DAPI
Fluorescent intensity (%)
Distance (μm)
RFP-Rab1b
BiP
DAPI
C
p < 0.001
Distance from BiP (μm)
Arf1
Rab1b

Figure 14

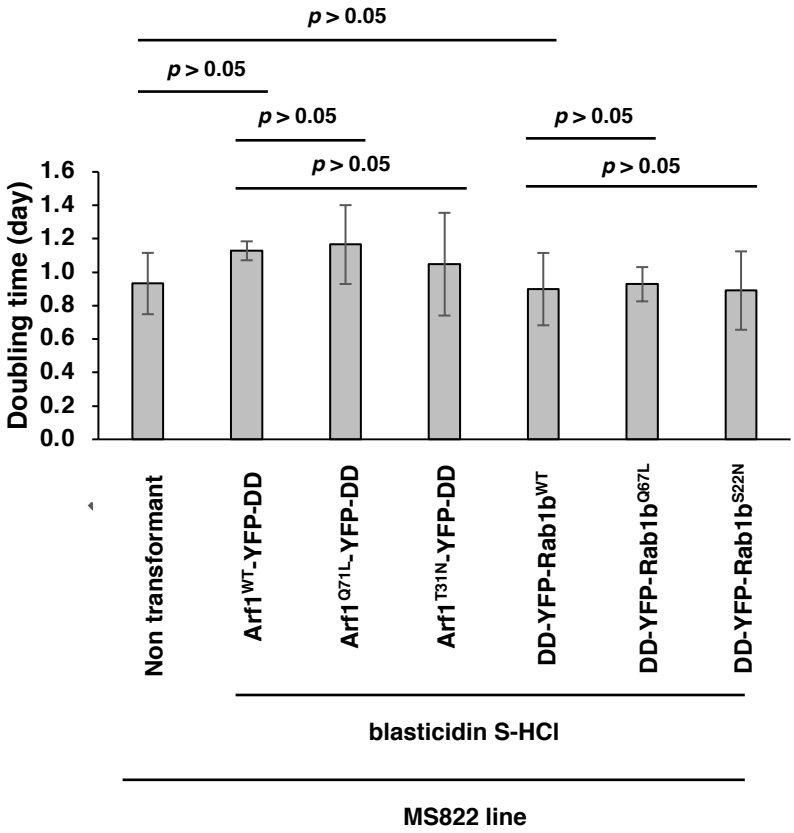
p > 0.05
p > 0.05
p > 0.05
p > 0.05
p > 0.05
p > 0.05
Doubling time (day)
1.6
1.4
1.2
1.0
0.8
0.6
0.4
0.2
0.0
Non transformant
Arf1WT-YFP-DD
Arf1Q71L-YFP-DD
Arf1T31N-YFP-DD
DD-YFP-Rab1bWT
DD-YFP-Rab1bQ67L
DD-YFP-Rab1bS22N
blasticidin S-HCl
MS822 line

Figure 15

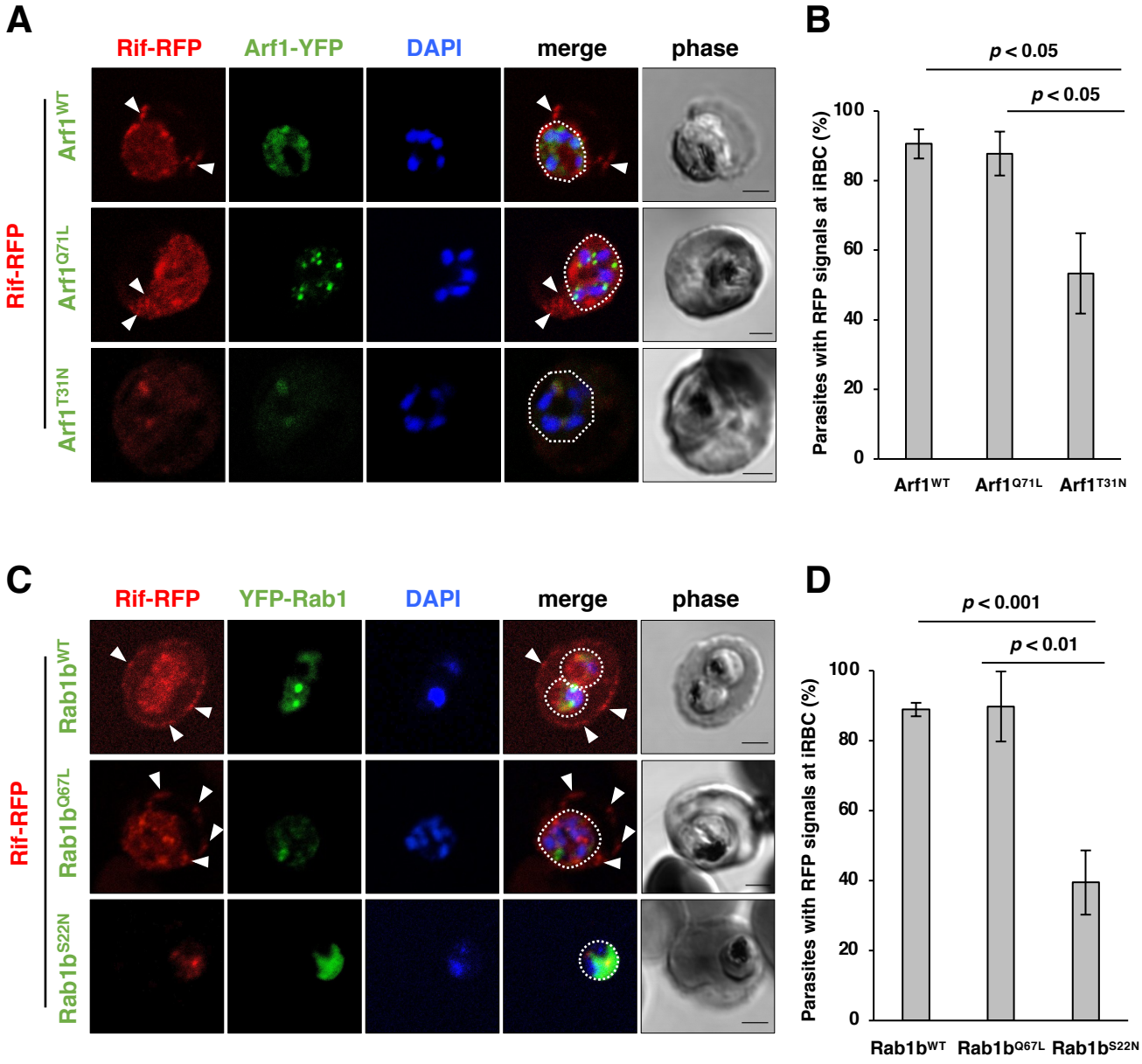
A
Rif-RFP
Arf1-YFP
DAPI
merge
phase
Rif-RFP
Arf1WT
Arf1Q71L
Arf1T31N
B
p < 0.05
p < 0.05
Parasites with RFP signals at iRBC (%)
100
80
60
40
20
0
Arf1WT
Arf1Q71L
Arf1T31N
C
Rif-RFP
YFP-Rab1
DAPI
merge
phase
Rif-RFP
Rab1bWT
Rab1bQ67L
Rab1bS22N
D
p < 0.001
p < 0.01
Parasites with RFP signals at iRBC (%)
100
80
60
40
20
0
Rab1bWT
Rab1bQ67L
Rab1bS22N

Figure 16

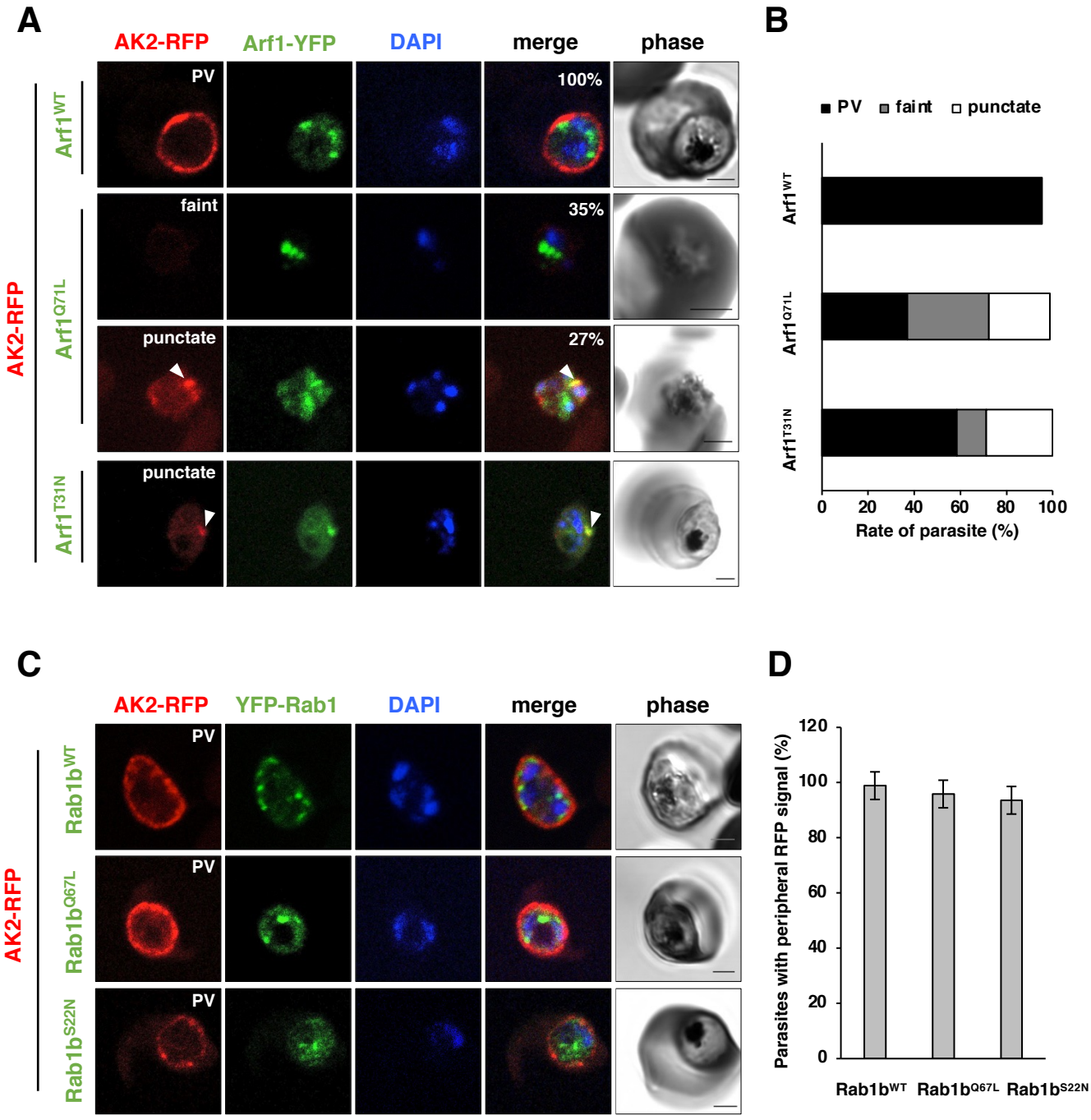
A
AK2-RFP
Arf1-YFP
DAPI
merge
phase
AK2-RFP
Arf1WT
Arf1Q71L
Arf1T31N
PV
100%
faint
35%
punctate
27%
punctate
B
PV
faint
punctate
Arf1WT
Arf1Q71L
Arf1T31N
0
20
40
60
80
100
Rate of parasite (%)
C
AK2-RFP
YFP-Rab1
DAPI
merge
phase
AK2-RFP
Rab1bWT
Rab1bQ67L
Rab1bS22N
PV
PV
PV
D
Parasites with peripheral RFP signal (%)
120
100
80
60
40
20
0
Rab1bWT
Rab1bQ67L
Rab1bS22N

Figure 17

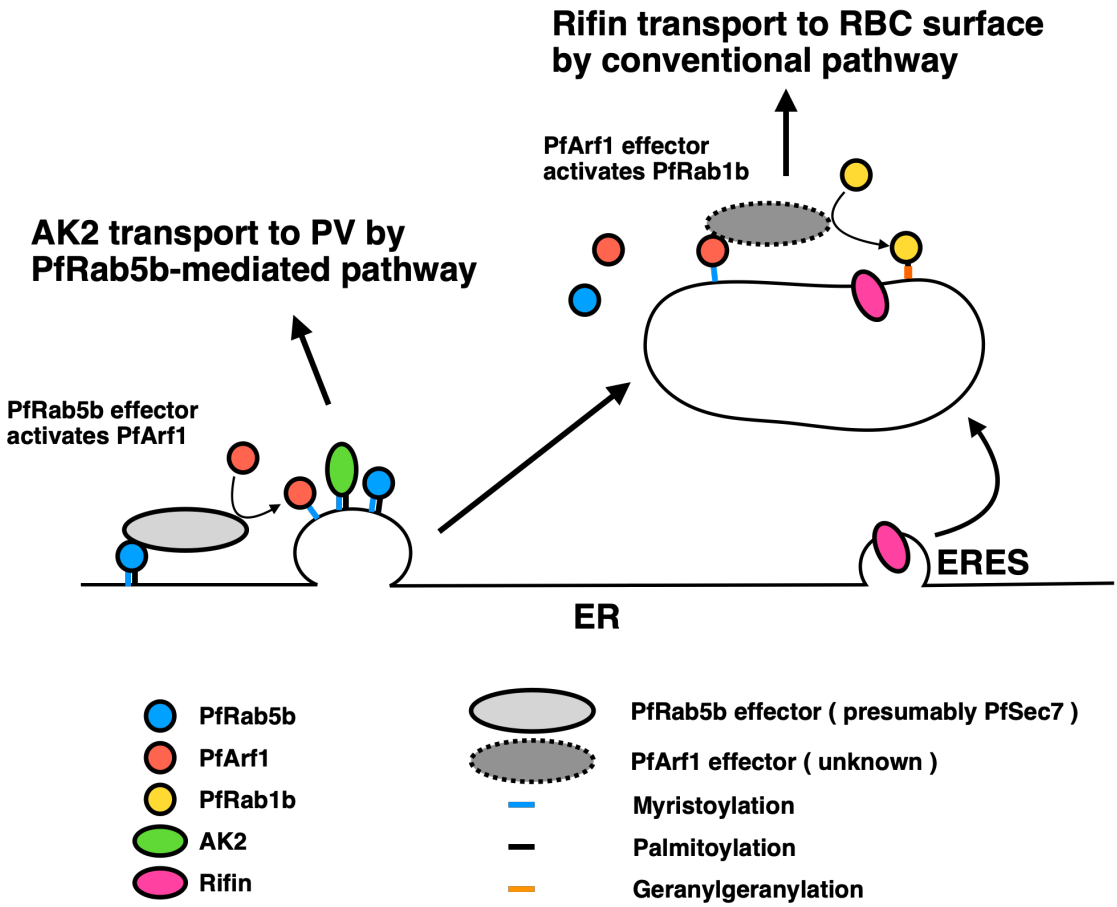
Rifin transport to RBC surface
by conventional pathway
PfArf1 effector
activates PfRab1b
AK2 transport to PV by
PfRab5b-mediated pathway
PfRab5b effector
activates PfArf1
ERES
ER
PfRab5b
PfArf1
PfRab1b
AK2
Rifin
PfRab5b effector (presumably PfSec7)
PfArf1 effector (unknown)
Myristoylation
Palmitoylation
Geranylgeranylation

Table 2

Sequences of the primers used in chapter 2.

construct	primer name	sequence
PfRab5b-YFP-FLAG	17-PfRGD2RFD-F	TATAAGGATCATGACATTGACTACAAAGACGATGACGACAAGACCCAGCTTTCTTGTACAAAGTGG
	18-PfRGD2RFD-R	AATGTCATGATCCTTATAATCTTCGTCATGGTCTTTGTAATCCATAGGATTGTTATAATATAAAACTTCTTTAAATCG
PbRab5b-YFP	19-PfGF-F	TATAAGGATCATGACATTGACTACAAAGACGATGACGACAAGTAGCTCGAGGGATATGGCAGC
	20-PfGF-R	AATGTCATGATCCTTATAATCTTCGTCATGGTCTTTGTAATCCATCTTGTACAGCTCGTCCATGC
PfArf1-RFP + PfRab5bQL-YFP-DD	pCen-Rab5b-GFP-DD-f	GCTTATAAATAAATAAAAATTTTATAAAACCATGGGATGTTCATCAAGCACCGAAAG
	pCen-Rab5b-GFP-DD-r	CGATGCAGTTTAGCGAACCAACATGTTTCCCCAATTTTTTTTTTTTTACC
	pCen-Arf1-RFP-f	GAGCGTGAGTTTTTTCTTTTCCCATATTTCCCCAATTTTTTTTTTTTTACCATTTTTTTATTAACC
	pCen-Arf1-RFP-r	GCTTATAAATAAATAAAAATTTTATAAAACATATGGGTTTATATGTAAGTAGGTTATTTAATCG
RFP-PfRab1b + PfRab5bQL-YFP-DD	pCen-Rab5b-GFP-DD-f	GCTTATAAATAAATAAAAATTTTATAAAACCATGGGATGTTCATCAAGCACCGAAAG
	pCen-Rab5b-GFP-DD-r	CGATGCAGTTTAGCGAACCAACATGTTTCCCCAATTTTTTTTTTTTTACC
	pCen-RFP-Rab1b-f	GAGCGTGAGTTTTTTCTTTTCCCATATTTCCCCAATTTTTTTTTTTTTACCATTTTTTTATTAACC
	pCen-RFP-Rab1b-r	GCTTATAAATAAATAAAAATTTTATAAAACATATGGTGTCTAAGGGCGAAGAGC
PfArf1-RFP	pCen-Arf1-RFP-f	GAGCGTGAGTTTTTTCTTTTCCCATATTTCCCCAATTTTTTTTTTTTTACCATTTTTTTATTAACC
	pCen-Arf1-RFP-r	GCTTATAAATAAATAAAAATTTTATAAAACATATGGGTTTATATGTAAGTAGGTTATTTAATCG
RFP-PfRab1b	pCen-RFP-Rab1b-f	GAGCGTGAGTTTTTTCTTTTCCCATATTTCCCCAATTTTTTTTTTTTTACCATTTTTTTATTAACC
	pCen-RFP-Rab1b-r	GCTTATAAATAAATAAAAATTTTATAAAACATATGGTGTCTAAGGGCGAAGAGC
PfArf1 (WT/QL/TN)-YFP-DD	CRT-Arf1-GFP-DD-DHFR-1	CTCGAGTTTGTTATATGTAAGAAATTAAAAAAAACAAAATAATAAATG
	CRT-Arf1-GFP-DD-DHFR-2	GTTTTTTTTAATTTCTTACATATAACAAACTCGAGATGGGTTTATATGTAAGTAGGTTATTT
	CRT-Arf1-GFP-DD-DHFR-3	TCGCCCTTGCTCACCATCTCGAGTTTGGCATTATTTAAGTGTGTGGTTAG
	CRT-Arf1-GFP-DD-DHFR-4	CTCGAGATGGTGAGCAAGGGCGA
	Arf1-GFP-DD-Q71L-f	GGAGGACtAGATAAGATCCGACCTTTATGG
	Arf1-GFP-DD-Q71L-r	CTTATCTaGTCCTCCTACATCCCATACGGT
	Arf1-GFP-DD-T31N-f	GGAAAAAaTACAATATTATATAAAGTAAAA
	Arf1-GFP-DD-T31N-r	TATTGTAtTTTTTCCAGCAGCATCTAATCC
DD-YFP-PfRab1b (WT/QL/SN)	GFP-Rab1bconnect-f	CCCAGCTTTCTTGTACAAAGTGGATGAATGATAGCTATGATAGTTTATTTAAAATATTG
	CRT-GFP-connect-r-yet	CCCTTGCTCACCATCTCGAGTTTGTTATATGTAAGAAATTAAAAAAAACAAAATAATAAATG
	Rab1b-DHFRconnect-r	AAAAACGAACATTAAGCTGCCATATCCTCAACAACATTTCTTTTTGGTATCCTTAATTG
	vector-DD-f	CATTCATTTATTATTTTGTTTTTTTTAATTTCTTACATATAACAAAATGGGAGTGCAGGTGGAAACC
	DD-GFP-r-yet	TCGCCCTTGCTCACCATCTCGAGTTCTTCCGGTTTTAGAAGCTCCAC
	Rab1b-S22N-r	CAAACAGTTTGATTTTCCAACACCACTAT
	Rab1b-S22N-f	GGAAAAAACTGTTTGCTCCTTCGTTTT
	Rab1b-Q67L-r	CCTTTCTAGCCCAGCCGTATC
	Rab1b-Q67L-f	GCTGGGCTAGAAAGGTTCCG
AK2-RFP	pC-AK2-RFP-forI-r	GCTTATAAATAAATAAAAATTTTATAAAACATATGGGATCATGTTATAGTAGAAAAAATAAAGTATC
	pC-AK2-RFP-forI-f	CTCCTTAATCAGCTCTTCGCCCTTAGACACATTGGGGTTATCATCTATAATGGAGC
Rifin-RFP	RifF1-RFP-connect-r	TCAGCTCTTCGCCCTTAGACACATCATTATTATAATTTGTCGATTGTGTGTC
	RFP-RifF2-connect-f	CTAGCAAACTGGGGCACAAACTTAAATTATTAGCAGAAAAAGTAGAAAAAGGTTG
	RifF2-PbDHFR3'-concect-r	CGAACATTAAGCTGCCATATCCATTTTATTGATTTAATAATTCTGTGTATTGGGC
	ef1-RifF1-conncect-r	GCTTATAAATAAATAAAAATTTTATAAAACATATGAAACTGCACTACACTAAAATATTATTATTTTTC

General Discussion

Through the identification of PfRab5b associate proteins, I revealed the novel mechanism which mediate export of N-myristoylated PfAK2 and PEXEL-positive Rifin to the periphery of parasite or erythrocyte cytosol by three small GTPases, PfRab5b, PfArf1 and PfRab1b with Sec7 which activate PfArf1, at adjacent to the ER in *Plasmodium falciparum*. The analysis of Sec7 in *P. falciparum* did not applicable due to technical difficulties, however, analysis of Sec7 in *P. berghei* showed the localization close to the ER and colocalization with PbRab5b (Figure 6 and 7D), supporting my hypothetical model that Sec7 plays as PfRab5b effector (Figure 17). Involvement of Arf and Rab GTPases in protein export at the ER, have not been reported in other eukaryotes including mammalian cells and budding yeast. My findings suggested the existence of unique mechanism for protein export in *Plasmodium* spp. and proposed the diversity of trafficking system mediated by Rab GTPases in eukaryotes.

N-acylated Rab5b showed unique features of membrane traffic in *Plasmodium* spp. C-terminal geranylgeranylated Rab5, referred as conventional Rab5, regulates endocytic transport in eukaryotic cells including land plants and *Apicomplexa* (Singer-Krüger et al., 1995; Kotzer et al., 2004; Elliott et al., 2008; Bottanelli et al., 2012; Kremer et al., 2013). In contrast, dual acylations, myristoylation and palmitoylation, at N-terminal Rab5 GTPase have been reported only in land plants (Ueda et al., 2001) and *Apicomplexan*

protists (Klöpper et al., 2012). N-acylated Rab5 isotype in *Arabidopsis thaliana*, ARA6/RabF1, localizes at the endosome and regulates transport from the endosome to the plasma membrane (Singer-Krüger et al., 1995; Ebine et al., 2011, 2012). Plant-unique Rab5 effector 2 (PUF2) is identified as an effector molecule of ARA6, and consequently the trafficking system mediated by ARA6 and PUF2 was elucidated (Ito et al., 2018, 2020). Either GTP-bound form of ARA6 or GDP-bound form of conventional Rab5 competitively binds to PUF2, and interacts with the common activating factor VPS9a, consequently ARA6 is negatively regulated by conventional Rab5 (Ito et al., 2018). In *Plasmodium falciparum*, N-acylated Rab5b localizes at adjacent to the ER, unlike the conventional Rab5 and plant ARA6 (Ebine et al., 2016). Interaction of PfRab5b with PfArf1, PfRab1b and Sec7, which is elucidated in this study, was *Plasmodium*-specific events, and indicated the presence of organism-specific trafficking systems around N-acylated Rab5 isotype. N-acylated Rab5b is also conserved in *Toxoplasma gondii*, another protozoan parasite of *Apicomplexa*, but TgRab5b localizes at early endosome with conventional Rab5 (TgRab5a, TgRab5c) (Kremer et al., 2013). TgRab5a and TgRab5c, but not TgRab5b, regulate vesicular transport from early endosome to microneme and rhoptry, that are unique secretory organelles in the parasite (Kremer et al., 2013). Further investigations to identify N-acylated Rab5-associate proteins in *Apicomplexa* are needed to clarify the diversity of trafficking systems regulated by N-acylated Rab5.

The plant-specific trafficking system based on N-acyrated ARA6, provides unique functions in salinity stress response (Ebine et al., 2011; Yin et al., 2017). Expression level of ARA6 is increased under the high-salt condition in halophytic plant *Mesembryanthemum crystallinum* (Bolte et al., 2000). In the loss of activity of ARA6 mutant, ara6-1, the growth was inhibited under the high-salt stress. While, overexpression of wild type and constitutively GTP-bound form ARA6 confer tolerance to high salinity on *Arabidopsis thaliana* (Ebine et al., 2011). In contrast, overexpression of ARA6 mutant with the deletion construct of N-terminus, does not affect the tolerance to salt stress, indicating that N-myrisoylation is indispensable for the salt tolerance (Yin et al., 2017). The function which is played by PfRab5b-mediated pathway still remain unclear. According to the essentiality of PbRab5b, it is expected that N-acylated Rab5 plays important role for parasite proliferation in asexual stage of *Plasmodium* parasites (Ezougou et al., 2014; Ebine et al., 2016). N-acylated protein, PfAK2, is transported to the parasite periphery by PfRab5b, however, neither PEXEL-positive protein EVP1 nor SBP1 which lacks N-acylation were regulated by PfRab5b (Ebine et al., 2016). N-terminal dual acylation might be a key to sort cargo proteins through the PfRab5b-mediated pathway. In *P. falciparum*, seventeen parasite proteins were reported as dual acylated except for PfAK2: calcium dependent protein kinase 1 (CDPK1) which localizes at PVM, glideosome associated protein 45 (GAP45) which localizes at inner membrane

complex and armadillo repeats-only protein (ARO) which localizes at rhoptry, etc. (Möskes et al., 2004; Cabrera et al., 2012; Ridzuan et al., 2012; Thavayogarajah et al., 2015). These dual acylated proteins might be the candidates of cargo protein for PfRab5b and the function of identified cargo proteins may shed light on the significance of PfRab5b-mediated pathway.

In conclusion, my results show that PfArf1 mediates the transport of N-myristoylated PfAK2 from the adjacent ER, and PfRab1b, which localizes differently than PfArf1, is involved in the export of PEXEL-positive Rifin to the erythrocyte cytosol. Currently, the mechanism how PfArf1 recognize cargo protein at the ER subdomain and sort to the pathway for the PVM, remains elusive. In other cases, there are very few reports on trafficking of dual acylated protein via a multivesicular body (Möskes et al., 2004; Shibata et al., 2017). In mammalian cells, myristoylated and palmitoylated GFP localized to the membrane subdomain enriched with cholesterol and ganglioside at the plasma membrane (McCabe and Berthiaume, 2001). It may plausible that PfArf1 together with PfRab5b and unidentified effector proteins organize the acylated cargo-recognition subdomain at the ER lipid subdomain. Consideration of the two facts that PfRab5b is essential for the growth (Ezougou et al., 2014; Ebine et al., 2016) and N- myristoyl transferase is a promising drug target for malaria (Schlott et al., 2018), suggests that elucidation of further molecular mechanism on PfArf1 and its regulatory proteins may help the *plasmodium*

biology as well as pathogenesis.

Acknowledgements

First of all, I would like to express my gratitude to my supervisor, Dr. Yumiko Saito-Nakano (National Institude of Infectious Diseases) for her advice on experimental design and useful discussions. I am grateful to Dr. Takeshi Annoura (National Institude of Infectious Diseases), Dr. Tamasa Araki (National Institude of Infectious Diseases) for helpful discussion and their technical support in experiments of *P. berghei*, kindly providing *P. berghei* Cl15Cy1 and UMV2 vector. I would like to thank Dr. Takashi Makiuchi (Tokai University), Dr. Naoaki Shinzawa (Tokyo Medical and Dental University), Prof. Shiroh Iwanaga (Osaka University), Mr. Tomohiro Hirai, Prof. Tomoyoshi Nozaki (The University of Tokyo) for their technical assistance and valuable discussion in experiment of *P. falciparum*. I thank Prof. Kiyoshi Kita (Nagasaki University) for providing the anti-PfBiP antibody, Prof. Osamu Kaneko (Nagasaki University) for the pCHD43(II) episomal plasmid, Daniel E Goldberg (Washington University School of Medicine) for the YFP-FKBP episomal plasmid, and Dr. Shunsuke Nakazawa (Nagasaki University) for kindly providing the *P. falciparum* MS822 line. The *P. falciparum* 3D7 line was obtained from MR4 (contributed by D. J. Carucci, MRA-102). Human RBCs and plasma were provided from the Japanese Red Cross Society and WR99210 was provided from Jacobus Pharmaceuticals.

Reference

Adisa, A., Albano, F. R., Reeder, J., Foley, M., and Tilley, L. (2001). Evidence for a role for a *Plasmodium falciparum* homologue of Sec31p in the export of proteins to the surface of malaria parasite-infected erythrocytes. *J. Cell Sci.* 114, 3377–3386.

Agop-Nersesian, C., Naissant, B., Rached, F. Ben, Rauch, M., Kretzschmar, A., Thiberge, S., et al. (2009). Rab11A-controlled assembly of the inner membrane complex is required for completion of *apicomplexan* cytokinesis. *PLOS Pathog.* 5, e1000270. doi:10.1371/journal.ppat.1000270.

Aikawa, M. (1971). Parasitological review. *Plasmodium*: the fine structure of malarial parasites. *Exp. Parasitol.* 30, 284–320. doi:10.1016/0014-4894(71)90094-4.

Akompong, T., Kadekoppala, M., Harrison, T., Oksman, A., Goldberg, D. E., Fujioka, H., et al. (2002). Trans expression of a *Plasmodium falciparum* histidine-rich protein II (HRPII) reveals sorting of soluble proteins in the periphery of the host erythrocyte and disrupts transport to the malarial food vacuole. *J. Biol. Chem.* 277, 28923–28933. doi:10.1074/jbc.M201968200.

Alexandre, J. S. F., Yahata, K., Kawai, S., Torii, M., and Kaneko, O. (2011). PEXEL-independent trafficking of *Plasmodium falciparum* SURFIN4.2 to the parasite-infected red blood cell and Maurer's clefts. *Parasitol. Int.* 60, 313–320. doi:10.1016/j.parint.2011.05.003.

Allan, B. B., Moyer, B. D., and Balch, W. E. (2000). Rab1 recruitment of p115 into a cis-SNARE complex: programming budding COPII vesicles for fusion. *Science (80-.).* 289, 444–448. doi:10.1126/science.289.5478.444.

Alvarez, C., Garcia-Mata, R., Brandon, E., and Sztul, E. (2003). COPI recruitment is modulated by a Rab1b-dependent mechanism. *Mol. Biol. Cell* 14, 2116–2127. doi:10.1091/mbc.e02-09-0625.

Appenzeller-Herzog, C., and Hauri, H. P. (2006). The ER-Golgi intermediate compartment (ERGIC): in search of its identity and function. *J. Cell Sci.* 119, 2173–2183. doi:10.1242/jcs.03019.

Armstrong, C. M., and Goldberg, D. E. (2007). An FKBP destabilization domain modulates protein levels in *Plasmodium falciparum*. *Nat. Methods* 4, 1007–1009. doi:10.1038/nmeth1132.

Barbieri, M. A., Li, G., Mayorga, L. S., and Stahl, P. D. (1996). Characterization of Rab5:Q79L-stimulated endosome fusion. *Arch Biochem Biophys* 326, 64–72. doi:8579373.

Barr, F. A. (2013). Review series: Rab GTPases and membrane identity: causal or inconsequential? *J. Cell Biol.* 202, 191–199. doi:10.1083/jcb.201306010.

Baumgartner, F., Wiek, S., Paprotka, K., Zauner, S., and Lingelbach, K. (2001). A point mutation in an unusual Sec7 domain is linked to brefeldin A resistance in a *Plasmodium falciparum* line generated by drug selection. *Mol. Microbiol.* 41,

1151–1158. doi:10.1046/j.1365-2958.2001.02572.x.

Benting, J., Ansorge, I., Paprotka, K., and Lingelbach, K. R. (1994a). Chemical and thermal inhibition of protein secretion have stage specific effects on the intraerythrocytic development of *Plasmodium falciparum* in vitro. *Tropocal Med. Parasitol.* 45, 303–307.

Benting, J., Mattei, D., and Lingelbach, K. (1994b). Brefeldin A inhibits transport of the glycophorin-binding protein from *Plasmodium falciparum* into the host erythrocyte. *Biochem J* 300, 821–826. doi:10.1042/bj3000821.

Bi, X., Mancias, J. D., and Goldberg, J. (2007). Insights into COPII Coat Nucleation from the Structure of Sec23•Sar1 Complexed with the Active Fragment of Sec31. *Dev. Cell* 13, 635–645. doi:10.1016/j.devcel.2007.10.006.

Boddey, J. A., Hodder, A. N., Günther, S., Gilson, P. R., Patsiouras, H., Kapp, E. A., et al. (2010). An aspartyl protease directs malaria effector proteins to the host cell. *Nature* 463, 627–631. doi:10.1038/nature08728.

Bolte, S., Schiene, K., and Dietz, K. J. (2000). Characterization of a small GTP-binding protein of the rab 5 family in *Mesembryanthemum crystallinum* with increased level of expression during early salt stress. *Plant Mol. Biol.* 42, 923–936. doi:10.1023/a:1006449715236.

Bottanelli, F., Gershlick, D. C., and Denecke, J. (2012). Evidence for sequential action of Rab5 and Rab7 GTPases in prevacuolar organelle partitioning. *Traffic2* 13, 338–

354. doi:10.1111/j.1600-0854.2011.01303.x.

Brandizzi, F., and Barlowe, C. (2013). Organization of the ER-Golgi interface for membrane traffic control. *Nat. Rev. Mol. Cell Biol.* 14, 382–392. doi:10.1038/nrm3588.

Bruce, M. C., Carter, R. N., Nakamura, K., Aikawa, M., and Carter, R. (1994). Cellular location and temporal expression of the *Plasmodium falciparum* sexual stage antigen Pfs16. *Mol Biochem Parasitol.* 65, 11–22. doi:10.1016/0166-6851(94)90111-2.

Cabrera, A., Herrmann, S., Warszta, D., Santos, J. M., Peter, A. T. J., Kono, M., et al. (2012). Dissection of minimal sequence requirements for rhoptry membrane targeting in the malaria parasite. *Traffic* 13, 1335–1350. doi:10.1111/j.1600-0854.2012.01394.x.

Cai, H., Yu, S., Menon, S., Cai, Y., Lazarova, D., Fu, C., et al. (2007). TRAPPI tethers COPII vesicles by binding the coat subunit Sec23. *Nature* 445, 941–944. doi:10.1038/nature05527.

Casanova, J. E. (2007). Regulation of Arf activation: the Sec7 family of guanine nucleotide exchange factors. *Traffic* 8, 1476–1485. doi:10.1111/j.1600-0854.2007.00634.x.

Chang, H. H., Falick, A. M., Carlton, P. M., Sedat, J. W., DeRisi, J. L., and Marletta, M. A. (2008). N-terminal processing of proteins exported by malaria parasites. *Mol.*

Biochem. Parasitol. 160, 107–115. doi:18534695.

Cherfils, J., Ménétrey, J., Mathieu, M., Le Bras, G., Robineau, S., Béraud-Dufour, S., et al. (1998). Structure of the Sec7 domain of the Arf exchange factor ARNO. *Nature* 392, 101–105. doi:10.1038/32210.

Collaborative, T. P. G. D. (2001). PlasmoDB: An integrative database of the *Plasmodium falciparum* genome. Tools for accessing and analyzing finished and unfinished sequence data. The *Plasmodium* Genome Database Collaborative. *Nucleic Acids Res.* 29, 66–69. doi:10.1093/nar/29.1.66.

Craig, E. A., Gambill, B. D., and Nelson, R. J. (1993). Heat shock proteins: molecular chaperones of protein biogenesis. *Microbiol. Rev.* 57, 402–414. doi:10.1128/mr.57.2.402-414.1993.

Crary, J. L., and Haldar, K. (1992). Brefeldin A inhibits protein secretion and parasite maturation in the ring stage of *Plasmodium falciparum*. *Mol. Biochem. Parasitol.* 53, 185–192. doi:10.1016/0166-6851(92)90020-k.

D'Souza-Schorey, C., and Chavrier, P. (2006). ARF proteins: Roles in membrane traffic and beyond. *Nat. Rev. Mol. Cell Biol.* 7, 347–358. doi:10.1038/nrm1910.

Dascher, C., and Balch, W. E. (1994). Dominant inhibitory mutants of ARF1 block endoplasmic reticulum to Golgi transport and trigger disassembly of the Golgi apparatus. *J. Biol. Chem.* 269, 1437–1448.

de Koning-Ward, T. F., Dixon, M. W. A., Tilley, L., and Gilson, P. R. (2016).

Plasmodium species: master renovators of their host cells. *Nat. Rev. Microbiol.* 14, 494–507. doi:10.1038/nrmicro.2016.79.

de Koning-Ward, T. F., Gilson, P. R., Boddey, J. A., Rug, M., Smith, B. J., Papenfuss, A. T., et al. (2009). A newly discovered protein export machine in malaria parasites. *Nature* 459, 945–949. doi:10.1038/nature08104.

Deitsch, K., Driskill, C., and Wellems, T. (2001). Transformation of malaria parasites by the spontaneous uptake and expression of DNA from human erythrocytes. *Nucleic Acids Res.* 29, 850–853. doi:10.1093/nar/29.3.850.

Der, C. J., Finkel, T., and Cooper, G. M. (1986). Biological and biochemical properties of human rasH genes mutated at codon 61. *Cell* 44, 167–176. doi:10.1016/0092-8674(86)90495-2.

Donaldson, J. G., and Jackson, C. L. (2011). ARF family G proteins and their regulators: Roles in membrane transport, development and disease. *Nat. Rev. Mol. Cell Biol.* 12, 362–375. doi:10.1038/nrm3117.

Ebine, K., Fujimoto, M., Okatani, Y., Nishiyama, T., Goh, T., Ito, E., et al. (2011). A membrane trafficking pathway regulated by the plant-specific RAB GTPase ARA6. *Nat. Cell Biol.* 13, 853–859. doi:10.1038/ncb2270.

Ebine, K., Hirai, M., Sakaguchi, M., Yahata, K., Kaneko, O., and Saito-Nakano, Y. (2016). *Plasmodium* Rab5b is secreted to the cytoplasmic face of the tubovesicular network in infected red blood cells together with N-acylated adenylate kinase 2.

Malar. J. 14. doi:10.1186/s12936-016-1377-4.

Ebine, K., Miyakawa, N., Fujimoto, M., Uemura, T., Nakano, A., and Ueda, T. (2012). Endosomal trafficking pathway regulated by ARA6, a RAB5 GTPase unique to plants. *Small GTPases* 3, 23–27. doi:10.4161/sgtp.18299.

Elliott, D. A., McIntosh, M. T., Hosgood, H. D. 3rd, Chen, S., Zhang, G., Baevova, P., et al. (2008). Four distinct pathways of hemoglobin uptake in the malaria parasite *Plasmodium falciparum*. *Proc Natl Acad Sci U S A.* 105, 2463–2468. doi:10.1073/pnas.0711067105.

Ellong, E. N., Soni, K. G., Bui, Q. T., Sougrat, R., Golinelli-Cohen, M. P., and Jackson, C. L. (2011). Interaction between the triglyceride lipase ATGL and the Arf1 activator GBF1. *PLoS One* 6, e21889. doi:10.1371/journal.pone.0021889.

Elmendorf, H. G., and Haldar, K. (1993). Identification and localization of ERD2 in the malaria parasite *Plasmodium falciparum*: separation from sites of sphingomyelin synthesis and implications for organization of the Golgi. *EMBO J.* 12, 4763–4773.

Elsworth, B., Matthews, K., Nie, C. Q., Kalanon, M., Charnaud, S. C., Sanders, P. R., et al. (2014). PTEX is an essential nexus for protein export in malaria parasites. *Nature* 511, 587–591. doi:10.1038/nature13555.

Eugster, A., Frigerio, G., Dale, M., and Duden, R. (2000). COP I domains required for coatomer integrity, and novel interactions with ARF and ARF-GAP. *EMBO J.* 19, 3905–3917. doi:10.1093/emboj/19.15.3905.

Ezougou, C. N., Ben-Rached, F., Moss, D. K., Lin, J. W., Black, S., Knuepfer, E., et al. (2014). *Plasmodium falciparum* Rab5B is an N-terminally myristoylated Rab GTPase that is targeted to the parasite's plasma and food vacuole membranes. *PLoS One* 9, e87695. doi:10.1371/journal.pone.0087695.

Feig, L. A., and Cooper, G. M. (1988). Inhibition of NIH 3T3 cell proliferation by a mutant ras protein with preferential affinity for GDP. *Mol. Biol. Cell* 8, 3235–3243. doi:10.1128/mcb.8.8.3235-3243.1988.

Franzusoff, A., Lauzé, E., and Howell, K. E. (1992). Immuno-isolation of Sec7p-coated transport vesicles from the yeast secretory pathway. *Nature* 355, 173–175. doi:10.1038/355173a0.

Gardner, M. J., Hall, N., Fung, E., White, O., Berriman, M., Hyman, R. W., et al. (2002). Genome sequence of the human malaria parasite *Plasmodium falciparum*. *Nature* 419, 498–511. doi:10.1038/nature01097.

Goldberg, J. (1998). Structural basis for activation of ARF GTPase: mechanisms of guanine nucleotide exchange and GTP-myristoyl switching. *Cell* 95, 237–248. doi:10.1016/s0092-8674(00)81754-7.

Goldberg, J. (2000). Decoding of sorting signals by coatomer through a GTPase switch in the COPI coat complex. *Cell* 100, 671–679. doi:10.1016/s0092-8674(00)80703-5.

Grebe, M., Gadea, J., Steinmann, T., Kientz, M., Rahfeld, J. U., Salchert, K., et al.

(2000). A conserved domain of the *arabidopsis* GNOM protein mediates subunit interaction and cyclophilin 5 binding. *Plant Cell* 12, 543–556. doi:10.1105/tpc.12.3.343.

Gustafson, M. A., and Fromme, J. C. (2017). Regulation of Arf activation occurs via distinct mechanisms at early and late Golgi compartments. *Mol. Biol. Cell* 28, 3660–3671. doi:10.1091/mbc.E17-06-0370.

Haubruck, H., and McCormick, F. (1991). Ras p21: effects and regulation. *Biochim Biophys Acta* 1072, 215–229. doi:10.1016/0304-419x(91)90015-d.

Hiller, N. L., Bhattacharjee, S., van Ooij, C., Liolios, K., Harrison, T., Lopez-Estraño, C., et al. (2004). A host-targeting signal in virulence proteins reveals a secretome in malarial infection. *Science (80-.).* 306, 1934–1937. doi:10.1126/science.1102737.

Hirai, T. (2016). Analysis of intracellular trafficking system regulated by PfRab5b GTPase, a unique small GTPase in *Plasmodium falciparum*, Master Thesis, School of life and environmental science, University of Tskuba, Ibaraki, Japan

Hsu, V. W., Shah, N., and Klausner, R. D. (1992). A brefeldin A-like phenotype is induced by the overexpression of a human ERD-2-like protein, ELP-1. *Cell* 69, 625–635. doi:10.1016/0092-8674(92)90226-3.

Hutagalung, A. H., and Novick, P. J. (2011). Role of Rab GTPases in membrane traffic and cell physiology. *Physiol. Rev.* 91, 119–149. doi:10.1152/physrev.00059.2009.

Iriko, H., Ishino, T., Tachibana, M., Omoda, A., Torii, M., and Tsuboi, T. (2020). Skeleton binding protein 1 (SBP1) of *Plasmodium falciparum* accumulates in electron-dense material before passing through the parasitophorous vacuole membrane. *Parasitol. Int.* 75. doi:10.1016/j.parint.2019.102003.

Ishizaki, R., Shin, H.-W., Iguchi-Ariga, S. M. M., Ariga, H., and Nakayama, K. (2006). AMY-1 (associate of Myc-1) localization to the trans-Golgi network through interacting with BIG2, a guanine-nucleotide exchange factor for ADP-ribosylation factors. *Genes Cells* 11, 949–959. doi:10.1111/j.1365-2443.2006.00991.x.

Ito, E., Choi, S. W., and Ueda, T. (2020). Purification and Interaction Analysis of a Plant-Specific RAB5 Effector by In Vitro Pull-Down Assay. *Methods Mol. Biol.* 2177, 183–197. doi:10.1007/978-1-0716-0767-1_15.

Ito, E., Ebine, K., Choi, S. W., Ichinose, S., Uemura, T., Nakano, A., et al. (2018). Integration of two RAB5 groups during endosomal transport in plants. *Elife* 7, e34064. doi:10.7554/eLife.34064.

Iwanaga, S., Kato, T., Kaneko, I., and Yuda, M. (2012). Centromere plasmid: a new genetic tool for the study of *Plasmodium falciparum*. *PLoS One* 7, e33326. doi:10.1371/journal.pone.0033326.

Jackson, C. L., and Casanova, J. E. (2000). Turning on ARF: the Sec7 family of guanine-nucleotide-exchange factors. *Trends Cell Biol.* 10, 60–67. doi:10.1016/s0962-8924(99)01699-2.

Janse, C. J., Ramesar, J., and Waters, A. P. (2006). High-efficiency transfection and drug selection of genetically transformed blood stages of the rodent malaria parasite *Plasmodium berghei*. *Nat. Protoc.* 1, 346–356. doi:10.1038/nprot.2006.53.

Joberty, G., Tavitian, A., and Zahraoui, A. (1993). Isoprenylation of Rab proteins possessing a C-terminal CaaX motif. *FEBS Lett.* 330, 323–328. doi:10.1016/0014-5793(93)80897-4.

Kaczmarek, B., Verbavatz, J. M., and Jackson, C. L. (2017). GBF1 and Arf1 function in vesicular trafficking, lipid homoeostasis and organelle dynamics. *Biol. cell* 109, 391–399. doi:10.1111/boc.201700042.

Kawamoto, K., Yoshida, Y., Tamaki, H., Torii, S., Shinotsuka, C., Yamashina, S., et al. (2002). GBF1, a guanine nucleotide exchange factor for ADP-ribosylation factors, is localized to the cis-Golgi and involved in membrane association of the COPI coat. *Traffic* 3, 483–495. doi:10.1034/j.1600-0854.2002.30705.x.

Kibria, K. M. K., Ferdous, J., Sardar, R., Panda, A., Gupta, D., Mohmmed, A., et al. (2019). A genome-wide analysis of coatomer protein (COP) subunits of apicomplexan parasites and their evolutionary relationships. *BMC Genomics* 20, 98. doi:10.1186/s12864-019-5463-1.

Klöpper, T. H., Kienle, N., Fasshauer, D., and Munro, S. (2012). Untangling the evolution of Rab G proteins: implications of a comprehensive genomic analysis. *BMC Biol.* 10, 71. doi:10.1186/1741-7007-10-71.

Kotzer, A. M., Brandizzi, F., Neumann, U., Paris, N., Moore, I., and Hawes, C. (2004). AtRabF2b (Ara7) acts on the vacuolar trafficking pathway in tobacco leaf epidermal cells. *J. Cell Sci.* 117, 6377–6389. doi:10.1242/jcs.01564.

Krai, P., Dalal, S., and Klemba, M. (2014). Evidence for a Golgi-to-endosome protein sorting pathway in *Plasmodium falciparum*. *PLoS One* 9, e89771. doi:10.1371/journal.pone.0089771.

Kremer, K., Kamin, D., Rittweger, E., Wilkes, J., Flammer, H., Mahler, S., et al. (2013). An overexpression screen of Toxoplasma gondii Rab-GTPases reveals distinct transport routes to the micronemes. *PLOS Pathog.* 9, e1003213. doi:10.1371/journal.ppat.1003213.

Kumar, N., Koski, G., Harada, M., Aikawa, M., and Zheng, H. (1991). Induction and localization of *Plasmodium falciparum* stress proteins related to the heat shock protein 70 family. *Mol Biochem Parasitol* 48, 47–58. doi:10.1016/0166-6851(91)90163-z.

Kumar, N., and Zheng, H. (1992). Nucleotide sequence of a *Plasmodium falciparum* stress protein with similarity to mammalian 78-kDa glucose-regulated protein. *Mol Biochem Parasitol* 56, 353–356. doi:10.1016/0166-6851(92)90187-o.

Kung, L. F., Pagant, S., Futai, E., D'Arcangelo, J. G., Buchanan, R., Dittmar, J. C., et al. (2012). Sec24p and Sec16p cooperate to regulate the GTP cycle of the COPII coat. *EMBO J.* 31, 1014–1027. doi:10.1038/emboj.2011.444.

Kurokawa, K., and Nakano, A. (2019). The ER exit sites are specialized ER zones for the transport of cargo proteins from the ER to the Golgi apparatus. *J. Biochem.* 165, 109–114. doi:10.1093/jb/mvy080.

Langreth, S. G., Jensen, J. B., Reese, R. T., and Trager, W. (1978). Fine structure of human malaria in vitro. *J. Protozool.* 25, 443–452. doi:10.1111/j.1550-7408.1978.tb04167.x.

Lanoix, J., Ouwendijk, J., Lin, C. C., Stark, A., Love, H. D., Ostermann, J., et al. (1999). GTP hydrolysis by arf-1 mediates sorting and concentration of Golgi resident enzymes into functional COP I vesicles. *EMBO J.* 18, 4935–4948. doi:10.1093/emboj/18.18.4935.

Lee, M. C. S., Moura, P. A., Miller, E. A., and Fidock, D. A. (2008). *Plasmodium falciparum* Sec24 marks transitional ER that exports a model cargo via a diacidic motif. *Mol. Microbiol.* 68, 1535–1546. doi:10.1111/j.1365-2958.2008.06250.x.

Lefrançois, S., and McCormick, P. J. (2007). The Arf GEF GBF1 is required for GGA recruitment to Golgi membranes. *Traffic2* 8, 144–1451. doi:10.1111/j.1600-0854.2007.00623.x.

Leung, K. F., Baron, R., and Seabra, M. C. (2006). Thematic review series: lipid posttranslational modifications. geranylgeranylation of Rab GTPases. *J. Lipid Res.* 47, 467–475. doi:16401880.

Lewis, M. J., and Pelham, H. R. (1990). A human homologue of the yeast HDEL

receptor. *Nature* 348, 162–163. doi:10.1038/348162a0.

Lewis, M. J., Sweet, D. J., and Pelham, H. R. (1990). The ERD2 gene determines the specificity of the luminal ER protein retention system. *Cell* 61, 1359–1363. doi:10.1016/0092-8674(90)90699-f.

Li, H., Adamik, R., Pacheco-Rodriguez, G., Moss, J., and Vaughan, M. (2003). Protein kinase A-anchoring (AKAP) domains in brefeldin A-inhibited guanine nucleotide-exchange protein 2 (BIG2). *Proc Natl Acad Sci U S A* 100, 1627–1632. doi:10.1073/pnas.0337678100.

Lin, J., Annoura, T., Sajid, M., Chevalley-Maurel, S., Ramesar, J., Klop, O., et al. (2011). A novel "gene insertion/marker out" (GIMO) method for transgene expression and gene complementation in rodent malaria parasites. *PLoS One* 6, e29289. doi:10.1371/journal.pone.0029289.

Mansour, S. J., Skaug, J., Zhao, X. H., Giordano, J., Scherer, S. W., and Melançon, P. (1999). p200 ARF-GEP1: a Golgi-localized guanine nucleotide exchange protein whose Sec7 domain is targeted by the drug brefeldin A. *Proc Natl Acad Sci U S A* 96, 7963–7973. doi:10.1073/pnas.96.14.7968.

Marti, M., Good, R. T., Rug, M., Knuepfer, E., and Cowman, A. F. (2004). Targeting malaria virulence and remodeling proteins to the host erythrocyte. *Science (80-.).* 306, 1930–1933. doi:10.1126/science.1102452.

Martinez, H., García, I. A., Sampieri, L., and Alvarez, C. (2016). Spatial-Temporal

Study of Rab1b Dynamics and Function at the ER-Golgi Interface. *PLoS One* 11, e0160838. doi:10.1371/journal.pone.0160838.

McCabe, J. B., and Berthiaume, L. G. (2001). N-terminal protein acylation confers localization to cholesterol, sphingolipid-enriched membranes but not to lipid rafts/caveolae. *Mol. Biol. Cell* 12, 3601–3617. doi:10.1091/mbc.12.11.3601.

McDonold, C. M., and Fromme, J. C. (2014). Four GTPases differentially regulate the Sec7 Arf-GEF to direct traffic at the trans-golgi network. *Dev. Cell* 30, 759–767. doi:10.1016/j.devcel.2014.07.016.

McGuffin, L. J., Bryson, K., and Jones, D. T. (2000). The PSIPRED protein structure prediction server. *Bioinformatics* 16, 404–405. doi:10.1093/bioinformatics/16.4.404.

Miller, L. H., Ackerman, H. C., Su, X., and Wellems, T. E. (2013). Malaria biology and disease pathogenesis: insights for new treatments. *Nat. Med.* 19, 156–67. doi:10.1038/nm.3073.

Ming, M., VanWye, J., Janse, C. J., Waters, A. P., and Haldar, K. (1999). Gene organization of rab6, a marker for the novel Golgi of *Plasmodium*. *Mol Biochem Parasitol* 100, 217–222. doi:10.1016/s0166-6851(99)00039-0.

Monetta, P., Slavin, I., Romero, N., and Alvarez, C. (2007). Rab1b interacts with GBF1 and modulates both ARF1 dynamics and COPI association. *Mol. Biol. Cell* 18, 2400–2410. doi:10.1091/mbc.e06-11-1005.

Morinaga, N., Tsai, S. C., Moss, J., and Vaughan, M. (1996). Isolation of a brefeldin A-inhibited guanine nucleotide-exchange protein for ADP ribosylation factor (ARF) 1 and ARF3 that contains a Sec7-like domain. *Proc Natl Acad Sci U S A* 93, 12856–12860. doi:10.1073/pnas.93.23.12856.

Morse, D., Webster, W., Kalanon, M., Langsley, G., and McFadden, G. I. (2016). *Plasmodium falciparum* Rab1A Localizes to Rhoptries in Schizonts. *PLoS One* 11, e0158174. doi:10.1371/journal.pone.0158174.

Möskes, C., Burghaus, P. A., Wernli, B., Sauder, U., Dürrenberger, M., and Kappes, B. (2004). Export of *Plasmodium falciparum* calcium-dependent protein kinase 1 to the parasitophorous vacuole is dependent on three N-terminal membrane anchor motifs. *Mol. Microbiol.* 54, 676–691. doi:10.1111/j.1365-2958.2004.04313.x.

Mossessova, E., Gulbis, J. M., and Goldberg, J. (1998). Structure of the guanine nucleotide exchange factor Sec7 domain of human arno and analysis of the interaction with ARF GTPase. *Cell* 92, 415–423. doi:10.1016/s0092-8674(00)80933-2.

Mouratou, B., Biou, V., Joubert, A., Cohen, J., Shields, D. J., Geldner, N., et al. (2005). The domain architecture of large guanine nucleotide exchange factors for the small GTP-binding protein Arf. *BMC Genomics* 6, 20. doi:10.1186/1471-2164-6-20.

Moyer, B. D., Allan, B. B., and Balch, W. E. (2001). Rab1 interaction with a GM130 effector complex regulates COPII vesicle cis--Golgi tethering. *Traffic* 2, 268–276.

doi:10.1034/j.1600-0854.2001.1o007.x.

Nakayama, K. (2004). Membrane Traffic: Editorial Overview. *J Biochem* 136, 751–753. doi:10.1093/jb/mvh.

Nakazawa, S., Culleton, R., and Maeno, Y. (2011). In vivo and in vitro gametocyte production of *Plasmodium falciparum* isolates from Northern Thailand. *Int J Parasitol* 41, 317–323. doi:21110978.

Nickel, W., and Rabouille, C. (2009). Mechanisms of regulated unconventional protein secretion. *Nat. Rev. Mol. Cell Biol.* 10, 148–155. doi:10.1038/nrm2617.

Niu, T. K., Pfeifer, A. C., Lippincott-Schwartz, J., and Jackson, C. L. (2005). Dynamics of GBF1, a Brefeldin A-sensitive Arf1 exchange factor at the Golgi. *Mol. Biol. Cell* 16, 1213–1222. doi:10.1091/mbc.e04-07-0599.

Ogun, S. A., and Holder, A. A. (1994). *Plasmodium yoelii*: brefeldin A-sensitive processing of proteins targeted to the rhoptries. *Exp. Parasitol.* 79, 270–278. doi:10.1006/expr.1994.1090.

Padilla, P. I., Chang, M. J., Pacheco-Rodriguez, G., Adamik, R., Moss, J., and Vaughan, M. (2003). Interaction of FK506-binding protein 13 with brefeldin A-inhibited guanine nucleotide-exchange protein 1 (BIG1): effects of FK506. *Proc Natl Acad Sci U S A* 100, 2322–2327. doi:10.1073/pnas.2628047100.

Park, S. K., Hartnell, L. M., and Jackson, C. L. (2005). Mutations in a highly conserved region of the Arf1p activator GEA2 block anterograde Golgi transport but not

COPI recruitment to membranes. *Mol. Biol. Cell* 16, 3786–3799. doi:10.1091/mbc.e05-04-0289.

Pasqualato, S., Renault, L., and Cherfils, J. (2002). Arf, Arl, Arp and Sar proteins: a family of GTP-binding proteins with a structural device for "front-back" communication. *EMBO Rep.* 3, 1035–1041. doi:10.1093/embo-reports/kvf221.

Pereira-Leal, J. B., and Seabra, M. C. (2000). The mammalian Rab family of small GTPases: definition of family and subfamily sequence motifs suggests a mechanism for functional specificity in the Ras superfamily. *J. Mol. Biol.* 301, 1077–1087. doi:10.1006/jmbi.2000.4010.

Peyroche, A., Paris, S., and Jackson, C. L. (1996). Nucleotide exchange on ARF mediated by yeast Gea1 protein. *Nature* 384, 479–481. doi:10.1038/384479a0.

Pipaliya, S. V, Schlacht, A., Klinger, C. M., Kahn, R. A., and Dacks, J. (2019). Ancient complement and lineage-specific evolution of the Sec7 ARF GEF proteins in eukaryotes. *Mol. Biol. Cell* 30, 1846–1863. doi:10.1091/mbc.E19-01-0073.

Quevillon, E., Spielmann, T., Brahimi, K., Chattopadhyay, D., Yeramian, E., and Langsley, G. (2003). The *Plasmodium falciparum* family of Rab GTPases. *Gene* 306, 13–25. doi:10.1016/s0378-1119(03)00381-0.

Rached, F. B., Ndjembo-Ezougou, C., Chandran, S., Talabani, H., Yera, H., Dandavate, V., et al. (2012). Construction of a *Plasmodium falciparum* Rab-interactome identifies CK1 and PKA as Rab-effector kinases in malaria parasites. *Biol. cell*

104, 34–47. doi:10.1111/boc.201100081 Free PMC article.

Ramaen, O., Joubert, A., Simister, P., Belgareh-Touzé, N., Olivares-Sanchez, M. C., Zeeh, J.-C., et al. (2007). Interactions between conserved domains within homodimers in the BIG1, BIG2, and GBF1 Arf guanine nucleotide exchange factors. *J Biol Chem* 282, 28834–28842. doi:10.1074/jbc.M705525200.

Richardson, B. C., McDonold, C. M., and Fromme, J. C. (2012). The Sec7 Arf-GEF is recruited to the trans-Golgi network by positive feedback. *Dev. Cell* 22, 799–810. doi:10.1016/j.devcel.2012.02.006.

Ridzuan, M. A. M., Moon, R. W., Knuepfer, E., Black, S., Holder, A. A., and Green, J. L. (2012). Subcellular location, phosphorylation and assembly into the motor complex of GAP45 during *Plasmodium falciparum* schizont development. *PLoS One* 7, e33845. doi:10.1371/journal.pone.0033845.

Russo, I., Babbitt, S., Muralidharan, V., Butler, T., Oksman, A., and Goldberg, D. E. (2010). Plasmepsin V licenses *Plasmodium* proteins for export into the host erythrocyte. *Nature* 463, 632–636. doi:10.1038/nature08726.

Sager, G., Szul, T., Lee, E., Kawai, R., Presley, J. F., and Sztul, E. (2021). Modeling the dynamic behaviors of the COPI vesicle formation regulators, the small GTPase Arf1 and its activating Sec7 guanine nucleotide exchange factor GBF1 on Golgi membranes. *Mol. Biol. Cell* 32, 446–459. doi:10.1091/mbc.E20-09-0587.

Saraste, J., and Kuismanen, E. (1992). Pathways of protein sorting and membrane

traffic between the rough endoplasmic reticulum and the Golgi complex. *Semin Cell Biol* 3, 343–355. doi:10.1016/1043-4682(92)90020-v.

Sargeant, T. J., Marti, M., Caler, E., Carlton, J. M., Simpson, K., Speed, T. P., et al. (2006). Lineage-specific expansion of proteins exported to erythrocytes in malaria parasites. *Genome Biol.* 7, R12. doi:10.1186/gb-2006-7-2-r12.

Saridaki, T., Fröhlich, K. S., Braun-Breton, C., and Lanzer, M. (2009). Export of PfSBP1 to the *Plasmodium falciparum* Maurer's clefts. *Traffic* 10, 137–152. doi:10.1111/j.1600-0854.2008.00860.x.

Scales, S. J., Gomez, M., and Kreis, T. E. (2000). Coat proteins regulating membrane traffic. *Int Rev Cytol* 195, 67–144. doi:10.1016/s0074-7696(08)62704-7.

Schindelin, J., Arganda-Carreras, I., Frise, E., Kaynig, V., Longair, M., Pietzsch, T., et al. (2012). Fiji: an open-source platform for biological-image analysis. *Nat. Methods* 9, 676–682. doi:10.1038/nmeth.2019.

Schlott, A. C., Holder, A. A., and Tate, E. W. (2018). N-Myristoylation as a Drug Target in Malaria: Exploring the Role of N-Myristoyltransferase Substrates in the Inhibitor Mode of Action. *ACS Infect. Dis.* 4, 449–457. doi:10.1021/acsinfecdis.7b00203.

Semenza, J. C., Hardwick, K. G., Dean, N., and Pelham, H. R. (1990). ERD2, a yeast gene required for the receptor-mediated retrieval of luminal ER proteins from the secretory pathway. *Cell* 61, 1349–1357. doi:10.1016/0092-8674(90)90698-e.

Sewell, J. L., and Kahn, R. A. (1988). Sequences of the bovine and yeast ADP-ribosylation factor and comparison to other GTP-binding proteins. *Proc Natl Acad Sci U S A* 85, 4620–4624. doi:10.1073/pnas.85.13.4620.

Shibata, T., Hadano, J., Kawasaki, D., Dong, X., and Kawabata, S. I. (2017). *Drosophila* TG-A transglutaminase is secreted via an unconventional Golgi-independent mechanism involving exosomes and two types of fatty acylations. *J. Biol. Chem.* 292, 10723–10734. doi:10.1074/jbc.M117.779710.

Singer-Krüger, B., Stenmark, H., and Zerial, M. (1995). Yeast Ypt51p and mammalian Rab5: counterparts with similar function in the early endocytic pathway. *J. Cell Sci.* 108, 3509–3521.

Spielmann, T., Fergusen, D. J. P., and Beck, H. P. (2003). etramps, a new *Plasmodium falciparum* gene family coding for developmentally regulated and highly charged membrane proteins located at the parasite-host cell interface. *Mol. Biol. Cell* 14, 1529–1544. doi:10.1091/mbc.e02-04-0240.

Spielmann, T., and Gilberger, T. W. (2010). Protein export in malaria parasites: do multiple export motifs add up to multiple export pathways? *Trends Parasitol.* 26, 6–10. doi:10.1016/j.pt.2009.10.001.

Stafford, W. H., Stockley, R. W., Ludbrook, S. B., and Holder, A. A. (1996). Isolation, expression and characterization of the gene for an ADP-ribosylation factor from the human malaria parasite, *Plasmodium falciparum*. *Eur J Biochem* 242, 104–113.

doi:10.1111/j.1432-1033.1996.0104r.x.

Stalder, D., and Antonny, B. (2013). Arf GTPase regulation through cascade mechanisms and positive feedback loops. *FEBS Lett.* 587, 2028–2035. doi:10.1016/j.febslet.2013.05.015.

Stearns, T., Willingham, M. C., Botstein, D., and Kahn, R. A. (1990). ADP-ribosylation factor is functionally and physically associated with the Golgi complex. *Proc Natl Acad Sci U S A* 87, 1238–1242. doi:10.1073/pnas.87.3.1238.

Stenmark, H. (2009). Rab GTPases as coordinators of vesicle traffic. *Nat. Rev. Mol. Cell Biol.* 10, 513–525. doi:10.1038/nrm2728.

Stenmark, H., Parton, R. G., Steele-Mortimer, O., Lütcke, A., Gruenberg, J., and Zerial, M. (1994). Inhibition of rab5 GTPase activity stimulates membrane fusion in endocytosis. *EMBO J.* 13, 1287–1296.

Struck, N. S., Dias, S. de S., Langer, C., Marti, M., Pearce, J. A., Cowman, A. F., et al. (2005). Re-defining the Golgi complex in *Plasmodium falciparum* using the novel Golgi marker PfGRASP. *J. Cell Sci.* 118, 5603–5613. doi:10.1242/jcs.02673.

Struck, N. S., Herrmann, S., Schmuck-Barkmann, I., Dias, S. de S., Haase, S., Cabrera, A. L., et al. (2008). Spatial dissection of the cis- and trans-Golgi compartments in the malaria parasite *Plasmodium falciparum*. *Mol. Microbiol.* 67, 1320–1330. doi:10.1111/j.1365-2958.2008.06125.x.

Suda, Y., Kurokawa, K., and Nakano, A. (2018). Regulation of ER-Golgi transport

dynamics by GTPases in budding yeast. *Front. Cell Dev. Biol.* 5, 1–6. doi:10.3389/fcell.2017.00122.

Teal, S. B., Hsu, V. W., Peters, P. J., Klausner, R. D., and Donaldson, J. G. (1994). An activating mutation in ARF1 stabilizes coatomer binding to Golgi membranes. *J. Biol. Chem.* 269, 3135–3138.

Thavayogarajah, T., Gangopadhyay, P., Rahlfs, S., Becker, K., Lingelbach, K., Przyborski, J. M., et al. (2015). Alternative Protein Secretion in the Malaria Parasite *Plasmodium falciparum*. *PLoS One* 10, e0125191. doi:10.1371/journal.pone.0125191.

Tisdale, E. J., Bourne, J. R., Khosravi-Far, R., Der, C. J., and Balch, W. E. (1992). GTP-binding mutants of rab1 and rab2 are potent inhibitors of vesicular transport from the endoplasmic reticulum to the Golgi complex. *J. Cell Biol.* 119, 749–761. doi:10.1083/jcb.119.4.749.

Townsley, F. M., Frigerio, G., and Pelham, H. R. (1994). Retrieval of HDEL proteins is required for growth of yeast cells. *J. Cell Biol.* 127, 21–28. doi:10.1083/jcb.127.1.21.

Ueda, T., Yamaguchi, M., Uchimiya, H., and Nakano, A. (2001). Ara6, a plant-unique novel type Rab GTPase, functions in the endocytic pathway of *Arabidopsis thaliana*. *EMBO J.* 20, 4730–4741. doi:10.1093/emboj/20.17.4730.

van Ooij, C., Tamez, P., Bhattacharjee, S., Hiller, N. L., Harrison, T., Liolios, K., et al.

(2008). The malaria secretome: from algorithms to essential function in blood stage infection. *PLOS Pathog.* 4, e1000084. doi:10.1371/journal.ppat.1000084.

Viotti, C. (2016). ER to Golgi-Dependent Protein Secretion: The Conventional Pathway. *Methods Mol. Biol.* 1459, 3–29. doi:10.1007/978-1-4939-3804-9_1.

Walliker, D., Quakyi, I. A., Wellems, T. E., McCutchan, T. F., Szarfman, A., London, W. T., et al. (1987). Genetic analysis of the human malaria parasite *Plasmodium falciparum*. *Science (80-.).* 236, 1661–1666. doi:10.1126/science.3299700.

Wang, R., Wang, Z., Wang, K., Zhang, T., and Ding, J. (2016). Structural basis for targeting BIG1 to Golgi apparatus through interaction of its DCB domain with Arl1. *J. Mol. Cell Biol.* 8, 459–461. doi:10.1093/jmcb/mjw033.

Wang, T., Li, L., and Hong, W. (2017). SNARE proteins in membrane trafficking. *Traffic* 18, 767–775. doi:10.1111/tra.12524.

Watanabe, N., Nakada-Tsukui, K., and Nozaki, T. (2020). Two isotypes of phosphatidylinositol 3-phosphate-binding sorting nexins play distinct roles in trogocytosis in *Entamoeba histolytica*. *Cell. Microbiol.* 22, e13144. doi:10.1111/cmi.13144.

WHO (2020). World Malaria Report 2020. < https://www.who.int/publications/i/item/9789240015791>, final access on 3rd December 2021. ISBN 978-92-4-001579-1

Xu, K. F., Shen, X., Li, H., Pacheco-Rodriguez, G., Moss, J., and Vaughan, M. (2005).

Interaction of BIG2, a brefeldin A-inhibited guanine nucleotide-exchange protein, with exocyst protein Exo70. *Proc Natl Acad Sci U S A* 102, 2784–2789. doi:10.1073/pnas.0409871102.

Yamaji, R., Adamik, R., Takeda, K., Togawa, A., Pacheco-Rodriguez, G., Ferrans, V. J., et al. (2000). Identification and localization of two brefeldin A-inhibited guanine nucleotide-exchange proteins for ADP-ribosylation factors in a macromolecular complex. *Proc Natl Acad Sci U S A* 97, 2567–2572. doi:10.1073/pnas.97.6.2567.

Yano, K., Komaki-Yasuda, K., Kobayashi, T., Takemae, H., Kita, K., Kano, S., et al. (2005). Expression of mRNAs and proteins for peroxiredoxins in *Plasmodium falciparum* erythrocytic stage. *Parasitol. Int.* 54, 35–41. doi:10.1016/j.parint.2004.08.005.

Yarwood, R., Hellicar, J., Woodman, P. G., and Lowe, M. (2020). Membrane trafficking in health and disease. *Dis. Model. Mech.* 13. doi:10.1242/dmm.043448.

Yin, C., Karim, S., Zhang, H., and Aronsson, H. (2017). *Arabidopsis* RabF1 (ARA6) Is Involved in Salt Stress and Dark-Induced Senescence (DIS). *Int J Mol Sci* 18, 309. doi:10.3390/ijms18020309.

Yorimitsu, T., and Sato, K. (2012). Insights into structural and regulatory roles of Sec16 in COPII vesicle formation at ER exit sites. *Mol. Biol. Cell* 23, 2930–2942. doi:10.1091/mbc.E12-05-0356.

Zhang, X., and Wang, Y. (2016). GRASPs in Golgi Structure and Function. *Front Cell Dev Biol* 3, 84. doi:10.3389/fcell.2015.00084.

Zhao, L., Helms, J. B., Brunner, J., and Wieland, F. T. (1999). GTP-dependent binding of ADP-ribosylation factor to coatomer in close proximity to the binding site for dilysine retrieval motifs and p23. *J. Biol. Chem.* 274, 14198–14203. doi:10.1074/jbc.274.20.14198.

Zhao, X., Lasell, T. K. R., and Melançon, P. (2002). Localization of large ADP-ribosylation factor-guanine nucleotide exchange factors to different Golgi compartments: evidence for distinct functions in protein traffic. *Mol. Biol. Cell* 13, 119–133. doi:10.1091/mbc.01-08-0420.